DMD Fast Forward. Published on August 9, 2019 as DOI: 10.1124/dmd.118.085902
This article has not been copyedited and formatted. The final version may differ from this version.

Title page

Prediction of atorvastatin pharmacokinetics in high-fat diet and low-dose streptozotocin induced diabetic rats using a semi-physiologically based pharmacokinetic model involving both enzymes and transporters

Zhongjian Wang, Hanyu Yang, Jiong Xu, Kaijing Zhao, Yang Chen, Limin Liang, Ping Li, Nan Chen, Donghao Geng, Xiangping Zhang, Xiaodong Liu and Li Liu.

Center of Drug Metabolism and Pharmacokinetics, School of Pharmacy, China Pharmaceutical University, Nanjing, China. (Z.W., H.Y., J.X., K.Z., Y.C., L.L., P.L., N.C., D.G., X.Z., X.L., L.L.)

DMD Fast Forward. Published on August 9, 2019 as DOI: 10.1124/dmd.118.085902
This article has not been copyedited and formatted. The final version may differ from this version.

Running Title Page

Running title: PBPK predicts atorvastatin disposition in diabetic rats

Correspondence to:

Li Liu (liulee@yeah.net) and Xiaodong Liu (xdliu@cpu.edu.cn)

Phone: +86 25 8327 1006; Fax: +86 25 8327 1060;

Center of Drug Metabolism and Pharmacokinetics, School of Pharmacy, China Pharmaceutical University, No.24 Tongjia Lane, Nanjing 210009, China.

Statistics:

The number of text pages: 51

The number of tables: 6

The number of figures: 6

The number of references: 56

The number of words in Abstract: 249

The number of words in Introduction: 612

The number of words in Discussion: 1390

Abbreviations

Ator, atorvastatin；

$AUC_{0-\infty}$, area under the concentration-time curve from time zero to infinity;

BCRP/Bcrp, breast cancer resistance protein;

$CL_{int,up}$, intrinsic uptake clearance;

C_{max} , the maximum concentration;

CYP3A/Cyp3a, cytochrome P450 3A;

DMEM, dulbecco's modified eagle's medium;

FBG, fasting blood glucose;

f_u, unbound fraction in plasma;

HBSS, hank's balanced salt solution;

k_a and k_b, absorption and efflux rate constant;

K_m, Michaelis-Menten constant;

LC-MS, liquid chromatograph mass spectrometer;

MRT, the mean residence time;

Nar, naringin;

O/P-OH-Ator, ortho/para-hydroxy atorvastatin;

OATPs/Oatps, organic anion transporting polypeptides;

PBSF, physiological-based scaling factor;

P_{eff}, effective permeability;

P-gp, P-glycoprotein;

Pra, prazosin;

Rho123, rhodamine 123;

Semi-PBPK model, Semi-physiologically based pharmacokinetic model;

STZ, streptozotocin;

$T_{1/2}$, terminal half-life;

TC, triglyceride;

TG, total cholesterol;

V_{max}, the maximum metabolic velocity.

DMD Fast Forward. Published on August 9, 2019 as DOI: 10.1124/dmd.118.085902
This article has not been copyedited and formatted. The final version may differ from this version.

Abstract

Atorvastatin is a substrate of cytochrome P450 3a (Cyp3a), organic anion transporting polypeptides (Oatps), breast cancer resistance protein (Bcrp) and P-glycoprotein (P-gp). We aimed to develop a semi-physiologically based pharmacokinetic (semi-PBPK) model involving both enzyme and transporters for predicting contributions of altered function and expression of Cyp3a and transporters to atorvastatin transport in diabetic rats by combination of high-fat diet feeding and low-dose streptozotocin injection. Atorvastatin metabolism and transport parameters came from in situ intestinal perfusion, primary hepatocytes and intestinal/hepatic microsomes. Expressions and functions of these proteins and their contributions were estimated. The results showed that diabetes increased expression of hepatic Cyp3a, Oatp1b2 and P-gp, but decreased expression of intestinal Cyp3a, Oatp1a5 and P-gp. Expression and function of intestinal Bcrp were significantly decreased in 10-day diabetic rats but increased in 22-day diabetic rats. The developed semi-PBPK model was successfully used to predict atorvastatin pharmacokinetics following oral and intravenous dose to rats based on alterations in Cyp3a and transporters by diabetes. Contributions to oral atorvastatin pharmacokinetics were intestinal Oatp1a5<intestinal P-gp<intestinal Cyp3a<hepatic Cyp3a <hepatic Oatp1b2<intestinal Bcrp. Contributions of decreased expression and function of intestinal Cyp3a and P-gp by diabetes to oral atorvastatin plasma exposure were almost attenuated by increased expression and function of hepatic Cyp3a and Oatp1b2. Opposite alterations in oral plasma atorvastatin exposure between 10-day and 22-day diabetic rats may be explained by altered intestinal Bcrp. In conclusion, altered atorvastatin pharmacokinetics by diabetes was synergistic effects of altered intestinal/hepatic Cyp3a and transporters and could be predicted using the developed semi-PBPK.

Introduction

Diabetes mellitus is often accompanied by hypercholesterolemia, which becomes a main reason leading to cardiovascular morbidity and mortality. Statins, including atorvastatin (Ator), are frequently prescribed to diabetic patients to reduce the risk of cardiovascular complications. The beneficial effects of statins in the prevention of cardiovascular diseases for diabetic patients have been demonstrated by clinic trials (Sattar et al., 2010; Preiss et al., 2011). Ator is primarily metabolized to ortho-hydroxy atorvastatin (O-OH-Ator) and para-hydroxy atorvastatin (P-OH-Ator) by cytochrome P450 3A (CYP3A/Cyp3a). Moreover, Ator is also a substrate of some drug transporters such as organic anion transporting polypeptides (OATPs/Oatps), breast cancer resistance protein (BCRP/Bcrp) and P-glycoprotein (P-gp) (Lennernäs, 2003; Generaux et al., 2011; Kellick et al., 2014; Kellick, 2017). CYP3A, OATPs, P-gp and BCRP are expressed in both human liver and intestine. It is generally accepted that the main human OATP in intestine is OATP1A2, whose orthologues of rats is Oatp1a5, and that the main human OATPs in liver are OATP1B1 and OATP1B3, sharing rat orthologues Oatp1b2. Ator, following oral administration, is absorbed into enterocyte via passive process and OATP1A2/Oatp1a5-mediated uptake, metabolized to P-OH-Ator and O-OH-Ator by intestinal CYP3A/Cyp3a, pumped back to intestine lumen via intestinal P-gp and BCRP/Bcrp, or effluxed out of enterocyte to portal vein. In portal blood, Ator is transported into hepatocytes via OATP1B1 (and possible OATP1B3)/Oatp1b2 at basolateral membrane of hepatocytes, subsequently metabolized to P-OH-Ator and O-OH-Ator by hepatic CYP3A/Cyp3a. These metabolites and Ator were effluxed out of hepatocytes to bile or blood circulation. Thus, disposition of Ator is mainly attributed to overall synergistic effects of CYP3A/Cyp3a and these transporters in intestine and liver, i.e. interplay of enzymes and transporters in liver and intestine.

Clinical trials and animal experiments have demonstrated that diabetes alters the

pharmacokinetic behaviors of some drugs (Gilbert et al., 1998; Hu et al., 2011; Dostalek et al., 2012; Shu et al., 2016). Our previous studies demonstrated that the plasma exposures of Ator and simvastatin acid were significantly decreased in diabetic rats induced by high-fat diet and low-dose streptozotocin (STZ) injection, partly due to the up-regulated activities and expression of both hepatic Cyp3a and Oatp1b2 (Xu et al., 2014; Shu et al., 2016). Moreover, Oatp-mediated uptake, P-gp/Bcrp-mediated efflux and intestinal Cyp3a-catalyzed metabolism are also attributed to the intestinal absorption of Ator. More importantly, the expression and function of Cyp3a in intestine and liver of diabetic rats showed opposite alterations (Hu et al., 2011). For example, the expression and function of intestinal Cyp3a, P-gp and Bcrp were significantly down-regulated (Yu et al., 2010; Hu et al., 2011; Liu et al., 2012), On the contrary, expression and function of hepatic Cyp3a significantly up-regulated in diabetic rats (Shu et al., 2016). All these results indicated that the alterations in the intestinal absorption and metabolism also contributed to the altered pharmacokinetic behaviors of drugs and that altered pharmacokinetics by diabetes should be combined effects of the alterations in hepatic/intestinal Cyp3a and drug transporters.

The aim of the study was to develop a semi-physiologically based pharmacokinetic (semi-PBPK) model involving interplay of intestinal/hepatic Cyp3a and drug transporters for quantitatively predicting pharmacokinetic profiles of Ator in diabetic rats. The DM rats were induced by HFD feeding plus low-dose STZ injection. The parameters of Ator metabolism and transport as well as their alterations by diabetes came from in situ intestinal perfusion, primary hepatocytes and intestinal/hepatic microsomes. The predicted pharmacokinetic profiles were further validated using *in vivo* data from diabetic (DM) rats, high-fat diet (HFD) rats and normal control (CON) rats. Several evidences (Lucas and Foy, 1977; Granneman and Stricker, 1984) have demonstrated that diabetes also alters physiological parameters such as gastrointestinal transit rate and organ blood flow rate, which were also introduced to the semi-PBPK.

DMD Fast Forward. Published on August 9, 2019 as DOI: 10.1124/dmd.118.085902
This article has not been copyedited and formatted. The final version may differ from this version.

Materials and Methods

Chemicals

1'-hydroxylmidazolam and STZ were purchased from Sigma-Aldrich Co. (Shanghai, China). Atorvastatin, midazolam and repaglinide were obtained from the National Institute for the Control of Pharmaceutical and Biological Products (Beijing, China). Para-hydroxy atorvastatin (P-OH-Ator) calcium and ortho-hydroxy atorvastatin (O-OH-Ator) calcium were purchased from TLC Pharmaceutical Standards Ltd. (Aurora, Ontario, Canada). β-actin antibody was purchased from Bioworld (Louis Park, MN, USA). Mouse monoclonal Cyp3a1, Oatp1b2 (M-50), Oatp1a5 (H-82) and Bcrp (M-70) antibodies were purchased from Santa Cruz Technology (Santa Cruz, CA, USA). Mouse monoclonal antibody specific for P-gp (clone C219) was purchased from Calbiochem-Novabiochem (Seattle, WA, USA). All the other reagents were commercially available.

Animals

Male Sprague-Dawley rats were purchased from Sino-British Sipper & BK Lab Animal Ltd. (Shanghai, China), and housed in an environment of controlled temperature (22 ± 2 °C) and relative humidity (50% ± 5%) with 12 h light/darkness cycle. Water and food were allowed ad libitum. Animal experiments were carried out according to institutional guidelines for the care and the use of laboratory animals and approved by the Animal Ethics Committee of China Pharmaceutical University (No. CPU-PCPK-1631010070). Experimental procedures were conducted in accordance with the Guide for the Care and Use of Laboratory Animals published by the US National Institutes of Health.

Development of DM rats

DM rats were induced by high fat diet feeding plus low dose STZ intraperitoneal injection

according to the method described previously (Shu et al., 2016) (supplemental methods). We once investigated effect of diabetic progression on pharmacokinetics of atorvastatin following oral dose of atorvastatin using diabetic rats induced by combination of HFD feeding and low dose STZ. It was found that compared with CON rats, the DM rats on day 10 (termed as 10-day DM rats) following STZ injection showed significantly higher oral plasma exposure of Ator. On the contrary, the DM rats on day 22 (termed as 22-day DM rats) following STZ intraperitoneal injection showed significantly lower oral plasma exposure of Ator. Therefore, both 10-day DM rats and 22-day DM rats were used for the following studies. The age-matched HFD rats and the age-matched CON rats were served as the controls.

Ator metabolism in rat intestinal and hepatic microsomes

Ator is mainly metabolized to O-OH-Ator and P-OH-Ator by intestinal and hepatic Cyp3a. Here, Ator metabolism was also detected in hepatic and intestinal microsomes. The hepatic and intestinal microsomes from experimental rats were prepared according to the methods described previously (Hu et al., 2011). The incubation mixture consisted of 40 μL of rat hepatic microsomes (final level 0.2 mg/mL) or intestinal microsomes (final level 1 mg/mL), 40 μL of the NADPH-regenerating system (0.5 mM NADP, 10 mM glucose 6-phosphate, 1 U/mL glucose-6-phosphate dehydrogenase, and 5 mM $MgCl_2$), and phosphate buffer solution (PBS, pH=7.4) (final volume 200 μL). After a 10 min pre-incubation at 37 °C, the reaction was initiated by addition of 10 μL of Ator solution and incubated for 10 min. The reaction was terminated by adding 1 mL of ethyl acetate. The formations of O-OH-Ator and P-OH-Ator were measured by LC-MS method (Shu et al., 2016). All of the above microsomal incubation conditions were in the linear range of the reaction rate. The final concentrations of Ator were set to be 2.5, 5, 10, 20 and 40 μM., respectively. Formation of 1'-hydroxylmidazolam (1'-OH-MDZ) from midazolam (MDZ 10 μM) in intestinal and hepatic microsomes were also measured to further assess CYP3A activity following 15 min incubation using above incubation system.

Free fractions (f_{umic}) of Ator in intestinal and hepatic microsome systems were measured using ultrafiltration on centrifugal filters (YM-30, Merck Millipore Ltd. MA, U.S.A) and K_m values were corrected by f_{umic}.

Uptake and metabolism of Ator in primary rat hepatocytes

The isolation of primary rat hepatocytes was operated according to the method reported previously (Jia et al., 2014). The isolated hepatocytes (viability> 85%), assessed by trypan blue assay, were suspended in plating medium (DMEM containing 5% fetal bovine serum, 1 mM dexamethasone, and 4 mg/L insulin) at a density of 2.5×10^5 cells/mL. A 500 μL aliquot of the hepatocytes suspension was seeded in collagen-pre coated plates for each well. Following 4-h incubation in a humidified atmosphere containing 5% CO_2, and the hepatocytes were used for investigating Ator metabolism and uptake.

The primarily cultured hepatocytes of experimental rats were rinsed twice with 500 μL warm Hank's balanced salt solution (HBSS) and incubated with 500 μL of the same buffer for 5 min at 37 °C. For uptake, hepatocytes were incubated in 500 μL HBSS containing Ator (0.1, 0.5, 2, 10 and 40 μM, respectively) for 2 min, the reaction was terminated by washing three times with ice-cold HBSS. Intracellular concentrations of Ator in hepatocytes were measured by LC-MS method. Kinetics of Ator uptake was characterized by equation 1 (Vildhede et al., 2014):

$$V = \frac{V_{max} \times S}{K_m + S} + CL_{up,\,int,\,Pas} \times S \qquad (1)$$

Where V and $CL_{up,int,\,Pas}$ are initial uptake velocity and the clearance via passive diffusion, respectively. K_m and $V_{\max}$ are the Michaelis constant and the maximal uptake rate for the saturable uptake, respectively. Kinetic parameters were estimated using Phoenix WinNonlin 8.1 (Pharsight, St. Louis, MO). The $CL_{up,\,int,\,active}$ was defined as V_{max}/K_m and the total uptake clearance ($CL_{int,uptake}$) was calculated by $CL_{up,int,active}$ plus $CL_{up,\,int,Pas}$.

It is generally accepted that Ator uptakes in hepatocytes is mainly mediated by Oatp1b2. Rifampicin is a typical inhibitor of Oatp1b2. Several reports have demonstrated that 100 μM rifampicin could completely inhibit OATP1B1-mediated uptake of estradiol-17β-glucuronide (Gui et al., 2008), Oatp1b2-mediated uptake of rosuvastatin and olmesartan acid (Ishida et al., 2018). Ator uptakes in the primary hepatocytes of normal rats were also measured in the presence of Oatp1b2 inhibitor rifampicin (200 μM) to investigate contribution of Oatp1b2 to hepatic uptake of Ator. The Oatp1b2-mediated intrinsic uptake clearance ($CL_{int,up,Oatp1b2}$) of Ator was calculated using equation 1.

For metabolism, hepatocytes were incubated in 500 μL HBSS containing Ator (0.1, 0.5, 2, 10 and 40 μM, respectively) for 30 min. The reaction was terminated by rinsing three times with ice-cold HBSS. The formations of O-OH-Ator and P-OH-Ator were measured by LC-MS method. Formation of 1'-hydroxymidazolam from midazolam (10 μM) following 120 min incubation and 2 min uptake of repaglinide (20 μM) were used to index functions of hepatic Cyp3a and Oatp1b2, respectively.

Intestinal absorption of Ator in rats

In situ single-pass intestinal perfusion experiments were performed to evaluate intestinal absorption of Ator as well as functions of intestinal P-gp and Bcrp in DM rats according to the method described previously (Cummins et al., 2003; Doluisio et al., 2010; Zhong et al., 2016) (supplemental methods). The perfusion Krebs-Henseleit buffer containing tested agents (0.5 μM Ator, 0.5 μM prazosin or 0.5 μM rhodamine 123) pre-warmed at 37 ℃ was perfused at 0.2 mL/min for about 30 min until steady state. The outlet perfusate samples were collected every 15 min for 120 min. The areas of the perfused segments (A) were measured at the end of the experiment. The apparent effective permeability (P_{eff}, cm/min) was calculated according to the equation $P_{eff} = -Q \cdot ln(C_{out}/C_{in})/A$, where C_{out} and C_{in} were concentrations of the tested agents in

the output and input buffers, respectively. Q (mL/min) was the flow rate corrected using a gravimetric method (Zhong et al., 2016).

Contributions of Oapt1a5, Bcrp and P-gp to intestinal absorption of Ator in normal rats (weighing 230-250 g) were estimated using in situ single-pass intestinal perfusion in the presence of corresponding transporter inhibitors, respectively. The isolated jejunum of rats were perfused with perfusion buffer containing Ator (0.5 μM), Ator (0.5 μM) + verapamil (P-gp inhibitor, 200 μM), Ator (0.5 μM) + Ko143 (Bcrp inhibitor, 1 μM) and Ator (0.5 μM)+naringin (Oatp1a5 inhibitor, 200 μM), respectively. Concentrations of verapamil, Ko143 and naringin were cited from the previous reports (Jiang et al., 2015; Duan et al., 2017). Assuming that their effects were additive, the contribution of each transporter to intestinal absorption of Ator was estimated following equations (2 ~ 5):

$$P_{eff,ator} = P_{eff,Pas} + P_{eff,Oatp1a5} - P_{eff,P-gp} - P_{eff,Bcrp} \quad (2)$$

$$P_{eff,P-gp} = P_{eff,+ver} - P_{eff,ator} \quad (3)$$

$$P_{eff,Bcrp} = P_{eff,+Ko143} - P_{eff,ator} \quad (4)$$

$$P_{eff,Oatp1a5} = P_{eff,ator} - P_{eff,+Nar} \quad (5)$$

where $P_{eff,ator}$, $P_{eff,+ver}$, $P_{eff,+Ko143}$ and $P_{eff,+Nar}$ represent apparent effective permeability of Ator in rats without transporter inhibitor, with verapamil, Ko143 and naringin, respectively. $P_{eff,Pas}$, $P_{eff,Oatp1a5}$, $P_{eff,Bcrp}$ and $P_{eff,P\text{-}gp}$ represent P_{eff} values of Ator transported process, Oatp1a5-mediated Ator uptake, Bcrp-mediated Ator efflux and P-gp-mediated Ator efflux across apical membrane of enterocyte, respectively.

Development of a semi-PBPK model involving both metabolic enzyme and drug transporters

A semi-PBPK model involving both intestinal/hepatic metabolic enzyme and transporters

(Figure 1) was constructed to describe the pharmacokinetic profiles of Ator following oral or intravenous administration to CON, HFD and DM rats. The essential structure of the PBPK model included stomach, gut lumen, gut wall, portal vein, hepatic blood, hepatocytes and system compartments. The gut lumen and gut wall were anatomically divided into duodenum, jejunum, and ileum with corresponding compartment volume, luminal radius and transit time.

Stomach

Assuming that neither absorption nor metabolism occurred in stomach, the amount of drug (A_0) in the stomach was governed by the gastric emptying rate, i.e.

$$\frac{dA_0}{dt} = -k_0 \times A_0 \qquad (6)$$

where k_0 represents the gastric emptying rate constant.

Gut Lumen

Absorption of Ator was often involved in intestinal Bcrp, P-gp and Oatp1a5. Transport of Ator from gut lumen to enterocytes was assumed to be governed by diffusion process and Oatp1a5-mediated uptake (Generaux et al., 2011), whose transfer rate constant was termed as $k_{a,i}$. On the contrary, efflux of Ator from enterocytes into the lumen was mediated by intestinal P-gp and Bcrp (Generaux et al., 2011; Kellick et al., 2014), whose transfer rate constant was termed as $k_{b.i}$.

Expression of the intestinal P-gp, Bcrp and Oatp1a5 were often region-dependent. Relative expression of intestinal P-gp, Bcrp and Oatp1a5 progressively increased from proximal to distal regions (Kawase et al., 2009; MacLean et al., 2010; Yu et al., 2010). Therefore, relative scaling factors ($SC_{P\text{-}gp,i}$, $SC_{Bcrp,i}$ and $SC_{Oatp1a5,i}$) for P-gp, Bcrp and Oatp1a5 were incorporated into the current PBPK model to correct $P_{eff,P\text{-}gp}$, $P_{eff,Bcrp}$ and $P_{eff,Oatp1a5}$ in corresponding gut segment. In general, values of P_{eff} were often estimated using jejunum, thus, $P_{eff,P\text{-}gp,i}$, $P_{eff,Bcrp,i}$ and $P_{eff,Oatp1a5,i}$ in the other gut segment were estimated using $P_{eff,P\text{-}gp}$,

jejunum×$SC_{P\text{-}gp,i}$, $P_{eff,Bcrp,\ jejunum}$×$SC_{Bcrp,i}$ and $P_{eff,Oatp1a5,\ jejunum}$× $SC_{Oatp1a5,i}$, respectively. Assuming that the expression of jejunal P-gp, Bcrp and Oatp1a5 proteins were set to be 1, $SC_{P\text{-}gp,doudenu,}$: $SC_{P\text{-}gp,\ jejunum}$:$SC_{P\text{-}gp,\ ileum}$ were estimated to be 0.578:1:1.883 using our previous report (Yu et al., 2010); $SC_{Bcrp,doudenu,}$:$SC_{Bcrp,jejunum}$:$SC_{Bcrp,ileum}$ were calculated to be 0.399:1:0.878 according to previous report (Kawase et al., 2009); and $SC_{\ Oatp1a5,doudenu}$:$SC_{\ Oatp1a5,\ jejunum}$:$SC_{\ Oatp1a5,\ ileum}$ were estimated to be 0.84: 1:1.73 based on data reported by (MacLean et al., 2010).

Thus, the $k_{a,i}$ and $k_{b,i.}$ in the i^{th} gut lumen were estimated using equation 7 and 8, respectively:

$$k_{a,i} = 2 \times (P_{eff,Pas} + SC_{Oatp1a5,i} \times P_{eff,Oatp1a5}) / r_i \quad (7)$$

$$k_{b,i} = 2 \times (SC_{P-gp,i} \times P_{eff,P-gp} + SC_{Bcrp,i} \times P_{eff,Bcrp}) / r_i \quad (8)$$

where i = 1, 2 and 3 represent duodenum, jejunum and ileum, respectively. r_i represents the radius of the i^{th} gut lumen.

The drug amount (A_i) in the gut lumen was described by equation 9:

$$\frac{dA_i}{dt} = k_{i-1} \times A_{i-1} - k_i \times A_i - k_{a,i} \times A_i + k_{b,i} \times A_{i,gw} \times f_{ugut} \quad (9)$$

Where k_i and $A_{i,gw}$ represent transit rate constant and drug amount in the i^{th} enterocyte compartment, respectively; f_{ugut} represents the unbound drug fraction in the enterocytes and is assumed to be 1 (Yang et al., 2007; Guo et al., 2013).

Enterocyte Compartment

It was assumed that each luminal compartment was associated with a unique enterocyte compartment, with no transit of drug between adjacent enterocyte compartments. The drug amount in the i^{th} enterocyte compartment was illustrated by equation (10 ~ 11) :

$$\frac{dA_{i,gw}}{dt} = k_{a,i} \times A_i + Q_{i,gw} \times \frac{A_{c1}}{V_{c1}} - k_{b,i} \times A_{i,gw} \times f_{ugut} - Q_{i,gw} \times \frac{A_{i,gw}}{V_{i,gw} \times (K_{pgut}/R_B)} - CL_{int,gw,i} \times \frac{f_u \times A_{i,gw}}{V_{i,gw} \times K_{pgut}/R_B} \quad (10)$$

$$CL_{int,gw,i} = PBSF_{i,gw} \times \sum \frac{V_{\max,gw,j}}{K_{m,gw,j} \times fu_{at,gut} + A_{i,gw} \times f_u / (V_{i,gw} \times K_{pgut}/R_B)} \quad (11)$$

where $V_{i,gw}$, $Q_{i,gw}$, A_p, V_p and K_{pgut} represent the volume of the i^{th} enterocyte compartment, its blood flow, the drug amount in portal vein compartment, volume of portal vein respectively and intestine-to-plasma drug concentration ratio,. $K_{m,gw,j}$ and $V_{max,gw,j}$ are kinetic parameters for formation of O-OH-Ator (j=1) and P-OH-Ator (j=2) from Ator in intestinal microsomes. $PBSF_i$ is physiological-based scaling factor (microsome content) in the i^{th} enterocyte compartment. R_B is Ator blood/plasma ratio, which was set to be 1.5 (Paine et al., 2008). $fu_{at,gut}$ refers to the free fraction of atorvastatin in rat intestinal microsomes, which was measured to be 0.89±0.01.

Expression and activity of intestinal Cyp3a were also region-dependent (Takemoto et al., 2003; Mitschke et al., 2008). Here, Ator metabolism was documented in jejunal microsomes. Therefore, Ator metabolism in other gut segment was corrected by relative scaling factor (SC_{Cyp3a}). Relative activity of Cyp3a in jejunum was set to be 1, $SC_{Cyp3a,doudenu}$ and $SC_{Cyp3a,\ ileum}$ were estimated to be 1.293 and 0.742, respectively, based on the reported data (Takemoto et al., 2003).

Portal Vein

The drug amount in the portal vein was described by equation 12 :

$$\frac{dA_p}{dt} = \sum Q_{i,gw} \times \frac{A_{i,gw}}{V_{i,gw} \times (K_{pgut}/R_B)} + Q_4 \times \frac{A_{c1}}{V_{c1}} - Q_p \times \frac{A_p}{V_p} \quad (12)$$

where Q_p, A_{c1} and V_{c1} are the blood flow of portal vein, the drug amount and its apparent distribution volume in the system compartment, respectively.

Hepatic compartment

In general, hepatic clearance of some drugs including statins was often governed by hepatic uptake. Thus, a two compartment model consisting of hepatic blood and hepatocytes was used to illustrate disposition of drugs in liver, i.e.

in hepatic blood:

$$\frac{dA_{h,b}}{dt} = Q_p \times \frac{A_p}{V_p} + Q_{h,at} \times \frac{A_{c1}}{V_{c1}} - Q_h \times \frac{A_{h,b}}{V_{h,b} \times (K_{ph}/R_B)} - CL_{up,ce} \times \frac{A_{h,b}}{V_{h,b}} + CL_{ef,ce} \times \frac{A_{h,ce}}{V_{h,ce}} \quad (13)$$

in hepatocytes:

$$\frac{dA_{h,ce}}{dt} = CL_{up,ce} \times \frac{A_{h,b}}{V_{h,b}} - CL_{ef,ce} \times \frac{A_{h,ce}}{V_{h,ce}} - CL_{h,m} \times \frac{A_{h,ce} \times f_u}{V_{h,ce} \times K_{ph}/R_B} \quad (14)$$

$$CL_{h,met} = PBSF_h \times \sum \frac{V_{\max,h,j}}{K_{m,h,j} \times fu_{at,h} + A_{h,ce} \times f_u / (V_{h,ce} \times K_{ph}/R_B)} \quad (15)$$

where $A_{h,b}$, $A_{h,ce}$, $V_{h,b}$ and $V_{h,ce}$ represent the amount of drug in the liver blood and liver cell compartment, volume of the liver blood and liver cell compartment, respectively. $Q_{h,at}$ represents the blood flow of hepatic artery and Q_h=Q_{pv}+$Q_{h,at}$. f_u and K_{ph} represents the unbound drug fraction in the blood and the liver-to-blood concentration ratio, separately. $CL_{up,ce}$, $CL_{ef,ce}$ and $CL_{h,m}$ represent intrinsic clearances of Ator uptake, efflux and metabolism in hepatocytes, respectively. $K_{m,h,j}$ and $V_{max,h,j}$ are kinetic parameters for formation of O-OH-Ator (j=1) and P-OH-Ator (j=2) from Ator in hepatic microsomes, respectively. $PBSF_h$ is physiological-based scaling factor of metabolism in liver. $fu_{at,h}$ refers to the free fraction of atorvastatin in rat liver microsomes, which was measured to be 0.95±0.01.

System compartment and peripheral compartment

Assuming that urinary excretion of Ator was negligible, the drug kinetics in the compartment was described by equation 16 and 17:

$$\frac{dA_{c1}}{dt} = Q_h \times \frac{A_{h,b}}{V_{h,b} \times (K_{ph}/R_B)} + k_{21} \times A_{c2} - k_{12} \times A_{c1} - \left(Q_4 + Q_{h,at} + \sum Q_{i,gw}\right) \times \frac{A_{c1}}{V_{c1}} \quad (16)$$

$$\frac{dA_{c2}}{dt} = k_{12} \times A_{c1} - k_{21} \times A_{c2} \quad (17)$$

where A_{c2} and V_{c2} are the drug amount and its apparent distribution volume in the

peripheral compartment, k_{12} and k_{21} are the drug amount rate constant between peripheral compartment and system compartment; respectively.

Coding and solving of the PBPK model were conducted by Phoenix WinNonlin 8.1 (Pharsight, St. Louis, MO). Pharmacokinetic profiles of Ator in plasma of CON rats, HFD rats and DM rats following oral or intravenous administration were predicted. Pharmacokinetic parameters (such as C_{max}, T_{max}, MRT, $T_{1/2}$, $AUC_{0-\infty}$, CL/F, CL and Vss) of the predicted profiles were estimated using non-compartmental analysis.

Contribution of altered expression of transporters and Cyp3a in intestine and liver to Ator pharmacokinetics

The expression of transporters and Cyp3a in intestine and liver of rats were measured using Western blotting (Supplemental methods). Diabetes significantly altered function and expression of transporters and Cyp3a in intestine and liver of rats in a different manner. Here, we further investigated individual contribution of the altered expression of transporters and Cyp3a to Ator pharmacokinetics and their integrated effects according to their alterations under diabetic status.

Pharmacokinetics of Ator after oral administrations to rats

Pharmacokinetic profiles of Ator in experimental rats were documented following oral administration of Ator (10 mg/kg) to 10-day DM rats, 22-day DM rats, the CON rats and HFD rats. Blood samples (250 μL) were collected in microcentrifuge tubes containing heparin under light ether anesthesia via the oculi chorioideae vein at 5, 10, 20, 30, 45, 60, 120, 240 and 360 min postdose. After 3 or 4 samplings, the appropriate amount of normal saline was administered to the rats via the tail vein to compensate for blood loss. Plasma samples were obtained by centrifugation for 10 min and stored at -80°C until analysis.

Drug analysis

Concentrations of Ator, O-OH-Ator and P-OH-Ator in biological fluids were determined using an LC-MS method previously described (Shu et al., 2016). The linear ranges of Ator, O-OH-Ator and P-OH-Ator were 3.9-500 ng/mL in plasma and hepatocytes, and were 3.9-1000 ng/mL in microsomes. If the concentrations of analytes in biological matrix exceeded the upper limit of quantification, analysis was operated following dilution using the blank matrix.

Statistical analysis

All results were expressed as mean ± deviation (S.D.). Statistical differences among groups were evaluated using one-way of analysis of variance (ANOVA). If analysis results were significant, the differences between groups were estimated by using a Student–Newman–Keuls multiple-comparison post hoc test. $P < 0.05$ was regarded as statistically significant.

Results

Establishment of DM rats

Physiological and biochemical parameters in rats were measured on day 10 and 22 after STZ injection (Table 1). The results showed that compared with CON and HFD rats, DM rats displayed significant increases in fasting blood glucose (FBG), total cholesterol (TG), and triglyceride (TC) levels, and homeostasis model of assessment for insulin resistance index (HOMA-IR), accompanied by a reduction in body weight. The DM rats also developed diabetic symptoms such as polyuria, polydipsia, and polyphagia. These alterations confirmed that the established DM rats were considered as diabetic rats (Shu et al., 2016).

Ator metabolism in intestinal and hepatic microsomes and expression of Cyp3a protein

In intestine and liver of rats, Ator is mainly metabolized to O-OH-Ator and P-OH-Ator by Cyp3a. Formations of O-OH-Ator and P-OH-Ator from Ator in both hepatic and intestinal microsomes of the 10-day DM rats, the 22-day DM rats, the age-matched CON and HFD rats were measured (Supplemental Figure 1). The formations of the two metabolites in hepatic and intestinal microsomes were better described by Michaelis-Menten equation, and the corresponding kinetic parameters were estimated (Table 2). The results showed that V_{max} values of O-OH-Ator formation in intestine and liver of CON rats were significantly higher than those of P-OH-Ator, although their K_m values were similar, inferring that Ator was preferentially metabolized to O-OH-Ator. Moreover, affinities of intestinal Cyp3a to Ator were comparable to those of hepatic Cyp3a (Table 2), inferring that characteristics of intestinal and hepatic Cyp3a catalyzing Ator metabolism were identical.

It was found that compared with CON rats, diabetes significantly increased metabolite generation in hepatic microsomes. For example, the estimated V_{max} values for formation of O-OH-Ator and P-OH-Ator in hepatic microsomes of 10-day DM rats were 1.47- and 1.48-fold

of the age-matched CON rats, respectively, but K_m values in hepatic microsomes of DM rats and CON rats were comparable. Similar alterations in formation of the two metabolites were also found in hepatic microsomes of 22-day DM rats.

On the contrary, Ator metabolism significantly decreased in intestinal microsomes of DM rats. The estimated V_{max} values for formation of O-OH-Ator and P-OH-Ator in intestinal microsomes of the 10-day DM rats were significantly decreased to about 64% and 46% of CON rats, respectively, but their K_m values were not obviously affected. Remarkable decreases in the V_{max} values for formation of the two metabolites were also found in intestinal microsomes of the 22-day DM rats. Feeding with HFD also significantly decreased metabolism of Ator in intestine, but its extent was less than that of diabetes. The alterations in activities of hepatic and intestinal Cyp3a1 by diabetes were further confirmed by formation of 1'-OH-MDZ (Supplemental Figure 1)

Expression of intestinal and hepatic Cyp3a1 proteins were also measured (Figure 2). It was consistent with alterations in activities of hepatic and intestinal Cyp3a, that diabetes significantly upregulated expression of hepatic Cyp3a1 proteins, but significantly downregulated expression of intestinal Cyp3a1 proteins.

Intestinal absorption of Ator, function and expression of transporters related to Ator transport in intestine of rats

Jejunal absorption of Ator in rats was documented using in situ single-pass perfusion (Figure 3). Interestingly, the effects of diabetes mellitus on jejunal absorption of Ator were dependent on diabetic progression. 10-day diabetes significantly jejunal P_{eff} value of Ator, inducing about 1.8-folds of CON rats. On the contrary, 22-day diabetes remarkably decreased jejunal P_{eff} value of Ator by about 60% of CON rats.

P-gp, Bcrp and Oatp1a5 were considered to be involved in Ator transport across apical

membrane of enterocytes. The functions of jejunal Bcrp and P-gp were investigated using another batch of experimental rats. The results showed that both 10-day diabetes and 22-day diabetes significantly downregulated function of jejunal P-gp, evidenced by significantly increases in jejunal P_{eff} value of rhodamine 123. Importantly, the effects of diabetes mellitus on function of intestinal Bcrp were also dependent on diabetic progression. 10-day diabetes significantly downregulated function of intestinal Bcrp, leading to significant increase in jejunal P_{eff} value of prazosin to about 2-fold of CON rats. On the contrary, function of intestinal Bcrp in 22-day diabetes was remarkably upregulated. The measured jejunal P_{eff} value of prazosin in 22-day DM rats was only 35% of CON rats.

Expression of jejunal P-gp, Bcrp and Oatp1a5 proteins was also measured (Figure 2). It was found that diabetes significantly downregulated expression of intestinal P-gp and Oatp1a5. Expression of intestinal Bcrp were downregulated in 10-day DM rats, but upregulated in 22-day DM rats, which was consistent with alterations in function of intestinal Bcrp by diabetes.

Contributions of jejunal Bcrp, P-gp and Oatp1a5 to intestinal absorption of Ator in normal rats were estimated using corresponding transporter inhibitors Ko143 (1 μM), verapamil (100 μM) and nargin (200 μM). The jejunal P_{eff} values across intestine of normal control rats without transporter inhibitor, with transporter inhibitor verapamil, Ko143 and nargin were measured to be 3.90±0.65, 6.1±0.53, 10.33±1.51 and 2.91±0.21($\times 10^{-3}$) cm/min, respectively. Then, $P_{eff,Pas}$, $P_{eff,P\text{-}gp}$, $P_{eff,bcrp}$ and $P_{eff,Oatp1a5}$ were estimated (Table 4) using equation 2~5. The results showed that contribution of jejunal Oatp1a5 to intestinal uptake of Ator was slight (less than 7%). Intestinal uptake of Ator was mainly via passive process. About 70% of uptake of Ator in enterocytes was returned to intestinal lumen via P-gp and Bcrp. Contributions of jejunal Bcrp and P-gp to Ator efflux were about 75% and 25%, respectively.

Assuming that jejunal P_{eff} values of transporter-mediated transport were positively correlated to expression of its protein and that relative extent of alterations (folds) in expression

of the indicated protein were similar among the three intestinal regions. The P_{eff} values of Ator in duodenum, jejunum and ileum for transporter-mediated transport under diabetic status were calculated (Table 4) using $P_{eff,i}$ value of CON rats × relative expression(*RE*) of its protein to CON rats. The interindividual variability and intra-individual variability of Oatp1a5, P-gp and Bcrp protein levels existed, which were used for Monte Carlo analysis. Based on the Monte Carlo error transfer analysis, the errors of corresponding parameters were obtained using 20 simulations. The results showed that the predicted total P_{eff} values of Ator (P_{eff} = $P_{eff,Pas}$+$P_{eff,Oatp1a5}$-$P_{eff,P\text{-}gp}$-$P_{eff,Bcrp}$) in DM rats and HFD rats were in good agreement with observations, whose fold-errors were within 2 (Table 4).

Ator uptake and metabolism in primary rat hepatocytes

The Ator uptake by hepatocytes is considered to be the rate-determining process of hepatic elimination (Maeda et al., 2011; Yabe et al., 2011). The hepatic uptake of Ator in primary rat hepatocytes was investigated (Figure 4A and 4B). The Ator uptake in hepatocytes was characterized by active transport(i.e Michaelis-Menten kinetics) plus passive diffusion. And corresponding parameters were estimated (Table 3). The results showed that Ator uptake was mainly attributed to active transport, accounting for 94% of total Ator uptake. Diabetes significantly increased maximal uptake rate of Ator (V_{max}), leading to higher active uptake clearance ($CL_{up,int,active}$, $CL_{int,uptake}$) of Ator by hepatocyte. The estimated $CL_{int,uptake}$ of Ator in hepatocytes of the 10-day DM rats and the 22-day DM rats were 2.34-and 1.68- fold of CON rats, respectively. HFD feeding also significantly increased $CL_{int,uptake}$ of Ator in hepatocytes of rats.

Uptake of Ator by hepatocytes of rats is mainly mediated by Oatp1b2 (Grime et al., 2008). It was found that diabetes also remarkably increased hepatic Oatp1b2 protein expression, resulting in increased uptake of repaglinide, a typical probe of Oatp1b2, confirming induction

of hepatic Oatp1b2 function. Further study showed that diabetes increased expression of hepatic Oatp1b2 and P-gp both in 10-day and 22-day DM rats. However, diabetes only decreased expression of hepatic Bcrp protein in 10-day DM rats but not 22-day. It was also found that co-administration of rifampin decreased Ator uptake by 77% in normal rat hepatocytes, further demonstrating that Oatps mainly contributed to hepatic uptake of Ator. The hepatic uptake of Ator in DM rats and HFD rats were also predicted following correction of Oatp1b2 expression (Table 4). The predictions were also near to observations, whose fold-errors were within 2.

Ator metabolism in primary rat hepatocytes was also investigated (Figure 4). The results showed that diabetes significantly increased V_{max} and decreased K_m values, inducing remarkable increases in CL_{int} vaules (Table 3). HFD feeding also enhanced Ator metabolism in hepatocytes, but extent of increase was less than that of diabetes.

Prediction of Ator pharmacokinetics following oral or intravenous administration of Ator in DM rats, HFD and CON rats using the semi-PBPK model

The developed semi-PBPK model was applied to predict pharmacokinetic profiles following oral administration of Ator (10 mg/kg) to 10-day and 22-day DM rats, HFD rats. and CON rats based on parameters were listed in Table 2, 3, 4 and 5. The intrinsic clearance of efflux from hepatocytes ($CL_{eff,ce}$) was to be 6 % of the predicted $CL_{up,ce}$ according to Table 3. Ator was extensively metabolized, only trace amounts of Ator were detected in urine of rats (Black et al., 1999) and the clearance of Ator via bile was less than 7% of total clearance (Dong et al., 2008). Therefore, contributions of biliary and renal excretion to elimination of Ator were minor, which were not considered during the prediction. The PBPK model was also used to predict pharmacokinetic profiles following intravenous administration of Ator (2 mg/kg) to 22-day DM rats, HFD rats and CON rats. The predicted pharmacokinetic profiles (Figure 5) and

corresponding pharmacokinetic parameters (Table 6) were further compared with the measured data in the study or our previous report (Shu et al., 2016).

The results showed that the predicted plasma concentrations of Ator in these experimental rats were comparable to observations, the most of predictions were within 2-fold error of observations (Figure 5). The predicted pharmacokinetic parameters except $T_{1/2}$ and T_{max} using the developed PBPK model were also in good agreement with observations. All these results indicated that pharmacokinetic profiles of Ator following intravenous and oral administration in both DM rats and HFD rats were successfully predicted using both the semi-PBPK model and alterations in parameters related to metabolism and transport in intestine and liver.

It was consistent with observations that alterations in oral plasma exposure of Ator in rats were dependent on diabetic progression. The predicted C_{max} and AUC of 10-day DM rats were about 1.6- and 1.7-fold of CON rats, respectively, which were in line with observations(1.7-fold for C_{max} and 1.6-fold for AUC). The predicted C_{max} and AUC in 22-day DM rats were only 58.6% and 62.1% of CON rats, respectively, which were also close to the observations (0.6-fold for C_{max} and 0.6-fold for AUC). The predicted plasma concentrations of Ator following intravenous dose to 22-day DM rats were lower than those of CON rats, whose AUC was about 79% of CON rats.

The pharmacokinetic behaviors of O-OH-Ator and P-OH-Ator following oral administration of Ator to rats were also investigated. It was consistent with findings in Ator that 10-day DM rats showed increased plasma exposures of O-OH-Ator and P-OH-Ator, whose AUC were 1.5 and 1.4-fold of CON rats. On the contrary, AUC of O-OH-Ator and P-OH-Ator in 22-day DM rats were only 71% and 58% of CON rats, respectively. The extents of alterations in plasma exposure of metabolites by diabetes were in line with those of alterations in plasma exposure of Ator by diabetes, indicating that alterations in oral plasma exposures of Ator and its metabolites in DM rats were mainly attributed to alterations in intestinal absorption,

although the altered pharmacokinetic behavior of Ator following oral dose under diabetic status should be combined effects of the alterations in hepatic/intestinal Cyp3a and drug transporters.

Visual predictive checks (VPC) was further used for assessing accuracy of predictions. It was assumed that inter-individual variability existed in $P_{eff,Bcrp}$, $P_{eff,P\text{-}gp}$, $CL_{up,int}$,hepatic and intestinal metabolic velocity ($V_{max,h,j}$, $V_{max,gw,j}$) of atorvastastin. The interindividual variability and intra-individual variability of these parameters were estimated using exponential model and multiplicative residual error model. The mean values of corresponding parameters listed in Tables 2, 3 and 4 were regarded as typical values and were subsequently subjected to visual predictive checks using 1000 times of simulations. The 5, 50, and 95th percentiles of the Monte-Carlo simulations were plotted along with the observed data following oral administration to CON, HFD, 10-day DM and 22-day DM rats (Supplemental Figure 3), which demonstrated that the virtual trial simulation plots validated that good predictions were achieved by the PBPK model for each group. Mean±SD values of pharmacokinetic parameters were also estimated using another 20 sets of simulations (Table 6).

Contributions of alteration in intestinal/hepatic Cyp3a, transporters, gastrointestinal transit rate constant k and organ blood flow rate Q to oral pharmacokinetics of Ator in rats

The above results indicated that alterations in oral pharmacokinetics of Ator in rats induced by diabetes should be attributed to combinational effects of Cyp3a and corresponding transporters in intestine and liver. Thus, individual contributions of alterations in intestinal Cyp3a, intestinal P-gp, intestinal Bcrp, intestinal Oatp1a5, hepatic Oatp1b2 and hepatic Cyp3a were separately investigated. Variations of intestinal P-gp, intestinal Bcrp and intestinal Oatp1a5 were set to 0.5, 1.0 and 1.5-fold of normal rats and the variations of intestinal Cyp3a, liver Cyp3a, liver Oatp1b2 gastrointestinal transit rate constant k and organ blood flow rate Q

were set to be 0.5, 1 and 2-fold of normal rats according to alterations under diabetic status. The results showed that contributions of the alterations to oral pharmacokinetics of Ator were intestinal Oatp1a5<intestinal P-gp <intestinal Cyp3a<hepatic Cyp3a <hepatic Oatp1b2 <intestinal Bcrp (Supplemental Figure 2). It was consistent with our expectation that both gastrointestinal transit rate and organ blood flow rate also affected pharmacokinetic behaviors of Ator (Supplemental Figure 2). Contribution of intestinal Oatp1a5 was slight compared with other proteins. According to alterations in expression of Cyp3a and corresponding transporter protein under diabetic status, we further investigated the combined effects of alterations in expression of these targeted proteins (intestinal Cyp3a, intestinal P-gp, intestinal Bcrp, intestinal Oatp1a5, hepatic Oatp1b2 and hepatic Cyp3a). Five combinations were taken into consideration (Figure 6), i.e. Combination 1: decreases in intestinal P-gp and intestinal Cyp3a, expressions of other proteins were normal; Combination 2: increases in hepatic Cyp3a and Otap1b2, expressions of other proteins were normal; Combination 3: Combination 1+Combination 2, expression of intestinal Bcrp was normal; Combination 4: Combination 1+ Combination 2, and decreases in expression of intestinal Bcrp (mimicking 10-day DM rats); Combination 5: Combination 1+ Combination 2, and increases in expression of intestinal Bcrp(mimicking day 22 DM rats). These simulations were compared with those in normal rats. It was consistent with our expectations that impairment of intestinal P-gp and intestinal Cyp3a (Combination 1) increased oral plasma exposure of Ator. On the contrary, increases in hepatic Cyp3a and Oatp1b2 (Combination 2) decreased oral plasma exposure of Ator. Interestingly, contributions of decreases in expression and function of intestinal Cyp3a and P-gp to oral plasma exposure of Aotr were almost attenuated by increases in expression and function of both hepatic Cyp3a and Oatp1b2 (Combination 3). The downregulation of intestinal Bcrp (combination 4) increased oral plasma exposures, but upregulation of intestinal Bcrp (combination 5) decreased oral plasma exposures of Ator in rats. These results indicated that

DMD Fast Forward. Published on August 9, 2019 as DOI: 10.1124/dmd.118.085902
This article has not been copyedited and formatted. The final version may differ from this version.

opposite alterations in oral Ator pharmacokinetic profiles in plasma of 10-day DM rats and 22-day DM rats may be explained by the altered expression and function of intestinal Bcrp.

Discussion

It is generally accepted that in rats Ator metabolism is mainly mediated by Cyp3a. Drug transporters, such as Oatps, Bcrp and P-gp, mediate Ator transport in intestine and liver. The main findings were that oral plasma exposure of Ator was increased in 10-day DM rats but decreased in 22-day DM rats. It was also found that diabetes altered function and expression of intestinal/hepatic drug transporters and Cyp3a in a different manner, which upregulated expression of hepatic P-gp, Oatp1b2 and Cyp3a, but downregulated expression of intestinal P-gp, Oapt1a5 and Cyp3a. Moreover, alterations of intestinal Bcrp were dependent on diabetic progression. These results indicated that alterations in pharmacokinetic behaviors of Ator by diabetes should be attributed to the integrated effects of alterations in intestinal/hepatic Cyp3a and transporters. The aim of our study was to develop a semi-PBPK model involving enzyme and transporter turnover to predict pharmacokinetic profiles of Ator in DM rats. DM rats were induced by combination of low dose and high fat diet feeding. The developed DM rats displayed typical symptoms including high levels of FBG, TG, and TC, insulin resistance, polyuria, polydipsia and polyphagia.

In intestine, Ator is easily absorbed, but high expressions of intestinal Cyp3a, Bcrp and P-gp lead to low bioavailability of Ator. The expression and function of Cyp3a and transporters under diabetic status as well as their contributions to intestinal absorption of Ator were first investigated. It was consistent with our previous reports (Yu et al., 2010; Hu et al., 2011) that diabetes downregulated expression of intestinal Cyp3a1, Oatp1a5 and P-gp. In consistence, Ator metabolism in intestinal microsomes was impaired and intestinal permeability of rhodamin 123 (a P-gp substrate) significantly increased in DM rats. Interestingly, expression and function of intestinal Bcrp were significantly decreased in 10-day DM rats and increased in 22-day DM rats, which were in line with alterations in intestinal permeability of Ator and prazosin (a Bcrp substrate). However, the alterations in expression and function of intestinal

Cyp3a, P-gp, Bcrp and Oatp1a5 did not explain opposite alterations in oral plasma exposure of Ator in 10-day and 22-day DM rats.

In human, OATP1B1 is the primary transporter responsible for mediating hepatic uptake of Ator (Kalliokoski and Niemi, 2009). Although OATP1B3 and Na(+)-taurocholate co-transporting polypeptide also transport most statins into the liver, their roles in systemic clearance was minor due to lower expressions or activities of these transporters (Smith et al., 2005; Ogasawara et al., 2010). Moreover, canalicular membrane of hepatocytes expresses some efflux transporters such as BCRP, P-gp and multidrug resistance-associated protein 2 (MRP2), effluxing statins into bile. In rats, Ator first entered hepatocytes via Oatp1b2, orthologues of human OATP1B1 and OATP1B3, then was metabolized by Cyp3a. Thus, expression and function of haptic Cyp3a and Oatp1b2 were measured. It was consistent with our previous reports (Xu et al., 2014; Shu et al., 2016) that diabetes significantly increased expression and function of Cyp3a and Oatp1b2, enhancing Ator metabolism and uptake by hepatocytes. It was also found that diabetes increased expression of hepatic P-gp protein in rats. Unlike P-gp, expression of hepatic Bcrp was significantly decreased in 10-day DM rats, but expression of hepatic Bcrp was unaffected in 22-day DM rats. The alterations in expression and function of hepatic Cyp3a and Oatp1b2 by diabetes did not explain the opposite alterations in pharmacokinetic profiles of Ator between 10-day and 22-day DM rats. All these results indicated that it was impossible to explain the altered plasma exposure of Ator following oral dose only in consideration of single alteration in expression and function of hepatic or intestinal Cyp3a or drug transporters and that the alterations in oral plasma exposure of Ator should be attributed to interplay of Cyp3a and transporters in liver and intestine.

Recently, PBPK model involving both enzyme and drug transporter turnover has been used to successfully predict disposition of drugs (Rasool et al., 2015; Jiang et al., 2016; Hsueh et al., 2017; Ono et al., 2017) under diseases status including diabetes or drug-drug interaction

(Guo et al., 2013; Wang et al., 2013; Ono et al., 2017). The present study demonstrated that diabetes significantly altered expression and function of intestinal/hepatic Cyp3a1, P-gp, Bcrp and Oapts in a different manner. Therefore, a semi-PBPK model involving alterations in intestinal/hepatic Cyp3a, uptake transporters and efflux transporters was developed to predict pharmacokinetic profiles of Ator in DM rats. Contribution of each transporter to Ator transport in intestine and liver as well as their integrated effects were investigated using corresponding transporter inhibitors. The individual contribution of Cyp3a and transporter was also separately documented. In intestine, it was found that uptake of Ator into enterocytes was mainly mediated via passive mechanism and that the contribution of Oatp1a5 was minor (only 7%). However, about 70% of Ator entered into enterocytes was returned to gut lumen, which was mainly attributed to intestinal Bcrp. The alterations in P_{eff} of Ator by diabetes were negatively related to expression of intestinal Bcrp, further demonstrating roles of intestinal Bcrp in intestinal absorption of Ator. In liver, contributions of Oat1b2 to uptake of Ator were about 94% (Table 3). Biliary clearance of Ator in rats was reported to be less than 7% of total clearance (Dong et al., 2008), indicating that roles of hepatic P-gp and Bcrp in Ator elimination were negligible. It was assumed that the transporter-mediated transport was positively correlated to level of transporter protein and that the integrated effects on Ator transport were additive, and the parameters of Ator transport under diabetic status were predicted by correcting expression of transporter proteins. The predicted parameters were all consistent with observations. Then, pharmacokinetic profiles of Ator following oral or intravenous administration of Ator to DM rats were predicted using the developed semi-PBPK model. Monte Carlo analysis predictions were within 2 fold-errors of observations, indicating the successful prediction.

Contributions of alterations in intestinal/hepatic Cyp3a, transporters, gastrointestinal transit rate constant k and organ blood flow rate Q related to Ator metabolism and transport to oral plasma exposure of Ator in DM rats were separately investigated (Supplemental Figure 2

A-H). The estimated contributions to oral pharmacokinetics of Ator were intestinal Oatp1a5 < intestinal P-gp < intestinal Cyp3a < hepatic Cyp3a < hepatic Oatp1b2<intestinal Bcrp, indicating that the contribution of intestinal Oatp1a5 to oral plasma exposure of Ator was minor. Interestingly, contributions of the decreased expression and function of intestinal Cyp3a and P-gp by diabetes (Combination 1) to oral plasma exposure of Aotr might be almost attenuated by the increased expression and function of hepatic Cyp3a and Oatp1b2 (Combination 2) (Figure 6A and 6B). The increase in intestinal blood flow rate in early diabetic rats is also the main cause of Ator absorption. Alterations in oral plasma exposure of Ator in DM rats were consistent with alterations in function and expression of intestinal Bcrp function, indicating that the increases in oral plasma exposure of Ator in 10-day DM rats and the decrease in 22-day DM rats were likely explained by oppositely altered alterations in expression and function of intestinal Bcrp. The simulated pharmacokinetic profiles of Ator based on Combination 5 supported above deduction (Figure 6B).

It is noteworthy that diabetes also alters some physiological parameters such as gastrointestinal transit (Granneman and Stricker, 1984; Durmus-Altun et al., 2011), gastrointestinal blood flow (Lucas and Foy, 1977), hepatic blood flow, renal function and components/weight of adipose tissue. In addition, function and expression of other transporters such as Mrp2 (Mei et al., 2012) were affected by diabetes. All these may lead to alteration in pharmacokinetics of atorvastatin by diabetes, which needed further investigation.

In conclusion, diabetes altered function and expression of Cyp3a, P-gp and Oatps in intestine and liver of rats in a different manner, downregulating intestinal Cyp3a, P-gp and Oatp1a5, and upregulating hepatic Cyp3a, Oatp1b2 and P-gp. Expression of Bcrp were dependent on diabetes progression. Diabetes decreased expression of intestinal and hepatic Bcrp at early phase (10-day diabetes), but increased expression of intestinal Bcrp without altering expression of hepatic Bcrp at later phase (22-day diabetes) (Figure 6C). In consistence,

diabetes increased at early phase but decreased oral plasma exposure of Ator at later phase. Alterations in pharmacokinetic profiles of Ator by diabetes were the synergistic effects of the altered intestinal/hepatic Cyp3a and transporters, which could be predicted using a semi-PBPK involving Cyp3a and transporters. The current work in our laboratory can be applied to changes in the proportion of protein content to construct physiological pharmacokinetic models. Changes in the expression level of a particular protein can be used to predict changes in the pharmacokinetic behavior of the drug under disease conditions. The developed semi-PBPK is often linked to alterations in function and expression of enzymes and transporters by disease. Theoretically, the model may be applied to predict pharmacokinetic behavior of the other drugs by other diseases if alterations in expression and function of enzymes and transporters were available.

Acknowledgements

This study was supported by the National Natural Science Foundation of China (No 81573490, 81872930, 81473273 and 81673505), Natural Science Foundation of Jiangsu Province (BK20161457) and “Double First-Class” University project (CPU2018GY22).

DMD Fast Forward. Published on August 9, 2019 as DOI: 10.1124/dmd.118.085902
This article has not been copyedited and formatted. The final version may differ from this version.

Authorship Contributions

Participated in research design: Wang, Yang, L. Liu, and X. Liu.

*Conducted experiments:*Wang, Yang, Xu, Liang, Geng, and Zhang.

*Contributed new reagents or analytic tools:*Wang, Yang, Xu, Liang, Geng, and Zhang.

Performed data analysis: Wang, Yang, Y. Chen, Li, Geng, and X. Liu.

Wrote or contributed to the writing of the manuscript: Wang, Yang, Zhao, N. Chen, L. Liu, and X. Liu.

References:

Black AE, Hayes RN, Roth BD, Woo P, and Woolf TF (1999) Metabolism and excretion of atorvastatin in rats and dogs. Drug Metab Dispos **27:**916-923.

Blomhoff R, ., Rasmussen M, ., Nilsson A, ., Norum KR, Berg T, ., Blaner WS, Kato M, ., Mertz JR, Goodman DS, and Eriksson U, . (1985) Hepatic retinol metabolism. Distribution of retinoids, enzymes, and binding proteins in isolated rat liver cells. J Biol Chem **260:**13560-13565.

Cummins CL, Salphati L, Reid MJ, and Benet LZ (2003) In vivo modulation of intestinal CYP3A metabolism by P-glycoprotein: studies using the rat single-pass intestinal perfusion model. J Pharmacol Exp Ther **305:**306-314.

Davies B and Morris T (1993) Physiological Parameters in Laboratory Animals and Humans. Pharm Res **10:**1093.

DeSesso JM and Jacobson CF (2001) Anatomical and physiological parameters affecting gastrointestinal absorption in humans and rats. Food Chem Toxicol **39:**209-228.

Doluisio JT, Billups NF, Dittert LW, Sugita ET, and Swintosky JV (2010) Drug absorption. I. An in situ rat gut technique yielding realistic absorption rates. J Pharm Sci **58:**1196-1200.

Dong J, Yu X, Wang L, Sun YB, Chen XJ, and Wang GJ (2008) Effects of cyclosporin A and itraconazole on the pharmacokinetics of atorvastatin in rats. Acta Pharmacol Sin **29:**1247-1252.

Dostalek M, Akhlaghi F, and Puzanovova M (2012) Effect of diabetes mellitus on pharmacokinetic and pharmacodynamic properties of drugs. Clin Pharmacokinet **51:**481-499.

Duan C, Guo JM, Dai Y, and Xia YF (2017) The absorption enhancement of norisoboldine in the duodenum of adjuvant-induced arthritis rats involves the impairment of P-

glycoprotein. Biopharm Drug Disposition **38:**75-83.

Durmus-Altun G, Vatansever U, Arzu Vardar S, Altaner S, and Dirlik B (2011) Scintigraphic evaluation of small intestinal transit in the streptozotocin induced diabetic rats. *Hippokratia* **15:**262-264.

Generaux GT, Bonomo FM, Johnson M, and Doan KM (2011) Impact of SLCO1B1 (OATP1B1) and ABCG2 (BCRP) genetic polymorphisms and inhibition on LDL-C lowering and myopathy of statins. Xenobiotica **41:**639-651.

Gilbert RE, Cooper ME, and Krum H (1998) Drug administration in patients with diabetes mellitus. Safety considerations. Drug Saf **18:**441-455.

Granneman JG and Stricker EM (1984) Food intake and gastric emptying in rats with streptozotocin-induced diabetes. *Am J Physiol* **247:**R1054-1061.

Grime K, Webborn PJ, and Riley RJ (2008) Functional consequences of active hepatic uptake on cytochrome P450 inhibition in rat and human hepatocytes. Drug Metab Dispos **36:**1670-1678.

Gui C, Miao Y, Thompson L, Wahlgren B, Mock M, Stieger B, and Hagenbuch B (2008) Effect of pregnane X receptor ligands on transport mediated by human OATP1B1 and OATP1B3. Eur J Pharmacol **584:**57-65.

Guo H, Liu C, Li J, Zhang M, Hu M, Xu P, Liu L, and Liu X (2013) A mechanistic physiologically based pharmacokinetic-enzyme turnover model involving both intestine and liver to predict CYP3A induction-mediated drug-drug interactions. J Pharm Sci **102:**2819-2836.

Hatley OJD, Jones CR, Galetin A, and Rostami-Hodjegan A (2017) Optimization of intestinal microsomal preparation in the rat: A systematic approach to assess the influence of various methodologies on metabolic activity and scaling factors. Biopharm Drug Dispos **38:**187-208.

Hill MA and Larkins RG (1989) Alterations in distribution of cardiac output in experimental diabetes in rats. Am J Physiol **257:**H571-580.

Hsueh CH, Hsu V, Zhao P, Zhang L, Giacomini KM, and Huang SM (2017) PBPK Modeling of the Effect of Reduced Kidney Function on the Pharmacokinetics of Drugs Excreted Renally by Organic Anion Transporters. Clin Pharmacol Ther **69:**702.

Hu N, Xie S, Liu L, Wang X, Pan X, Chen G, Zhang L, Liu H, Liu X, Liu X, Xie L, and Wang G (2011) Opposite effect of diabetes mellitus induced by streptozotocin on oral and intravenous pharmacokinetics of verapamil in rats. Drug Metab Dispos **39:**419-425.

Ishida K, Ullah M, Toth B, Juhasz V, and Unadkat JD (2018) Transport Kinetics, Selective Inhibition, and Successful Prediction of In Vivo Inhibition of Rat Hepatic Organic Anion Transporting Polypeptides. Drug Metab Dispos **46:**1251-1258.

Jia LL, Zhong ZY, Li F, Ling ZL, Chen Y, Zhao WM, Li Y, Jiang SW, Xu P, Yang Y, Hu MY, Liu L, and Liu XD (2014) Aggravation of clozapine-induced hepatotoxicity by glycyrrhetinic acid in rats. J Pharmacol Sci **124:**468-479.

Jiang S, Zhao W, Chen Y, Zhong Z, Zhang M, Li F, Xu P, Zhao K, Li Y, Liu L, and Liu X (2015) Paroxetine decreased plasma exposure of glyburide partly via inhibiting intestinal absorption in rats. Drug Metab Pharmacokinet **30:**240-246.

Jiang X, Zhuang Y, Xu Z, Wang W, and Zhou H (2016) Development of a Physiologically Based Pharmacokinetic Model to Predict Disease-Mediated Therapeutic Protein-Drug Interactions: Modulation of Multiple Cytochrome P450 Enzymes by Interleukin-6. AAPS J **18:**767-776.

Kalliokoski A and Niemi M (2009) Impact of OATP transporters on pharmacokinetics. Br J Pharmacol **158:**693-705.

Kawase A, Matsumoto Y, Hadano M, Ishii Y, and Iwaki M (2009) Differential effects of chrysin on nitrofurantoin pharmacokinetics mediated by intestinal breast cancer resistance

protein in rats and mice. J Pharm Pharm Sci **12:**150-163.

Kellick K (2017) Organic Ion Transporters and Statin Drug Interactions. Curr Atheroscler Rep **19:**65.

Kellick KA, Bottorff M, and Toth PP (2014) A clinician's guide to statin drug-drug interactions. J Clin Lipidol **8:**S30-S46.

Kimura T and Higaki K (2002) Gastrointestinal transit and drug absorption. Biol Pharm Bull **25:**149.

Lennernäs H (2003) Clinical pharmacokinetics of atorvastatin. Clin Pharmacokinet **42:**1141.

Liu H, Liu L, Li J, Mei D, Duan R, Hu N, Guo H, Zhong Z, and Liu X (2012) Combined contributions of impaired hepatic CYP2C11 and intestinal breast cancer resistance protein activities and expression to increased oral glibenclamide exposure in rats with streptozotocin-induced diabetes mellitus. Drug Metab Dispos **40:**1104-1112.

Lucas PD and Foy JM (1977) Effects of experimental diabetes and genetic obesity on regional blood flow in the rat. Diabetes **26:**786-792.

MacLean C, Moenning U, Reichel A, and Fricker G (2010) Regional absorption of fexofenadine in rat intestine. Eur J Pharm Sci **41:**670-674.

Maeda K, Ikeda Y, Fujita T, Yoshida K, Azuma Y, Haruyama Y, Yamane N, Kumagai Y, and Sugiyama Y (2011) Identification of the rate-determining process in the hepatic clearance of atorvastatin in a clinical cassette microdosing study. Clin Pharmacol Ther **90:**575-581.

Mei D, Li J, Liu H, Liu L, Wang X, Guo H, Liu C, Duan R, and Liu X (2012) Induction of multidrug resistance-associated protein 2 in liver, intestine and kidney of streptozotocin-induced diabetic rats. *Xenobiotica* **42:**709-718.

Mitschke D, Reichel A, Fricker G, and Moenning U (2008) Characterization of cytochrome P450 protein expression along the entire length of the intestine of male and female rats.

Drug Metab Dispos **36:**1039-1045.

Naritomi Y, Terashita S, Kagayama A, and Sugiyama Y (2003) Utility of hepatocytes in predicting drug metabolism: comparison of hepatic intrinsic clearance in rats and humans in vivo and in vitro. Drug Metab Dispos **31:**580-588.

Ogasawara K, Terada TT, Hatano E, Ikai I, Yamaoka Y, and Inui K (2010) Hepatitis C virus-related cirrhosis is a major determinant of the expression levels of hepatic drug transporters. Drug Metab Pharmacokinet **25:**190-199.

Ono C, Hsyu PH, Abbas R, Loi CM, and Yamazaki S (2017) Application of Physiologically Based Pharmacokinetic Modeling to the Understanding of Bosutinib Pharmacokinetics: Prediction of Drug-Drug and Drug-Disease Interactions. Drug Metab Dispos **45:**390-398.

Paine SW, Parker AJ, Gardiner P, Webborn PJ, and Riley RJ (2008) Prediction of the pharmacokinetics of atorvastatin, cerivastatin, and indomethacin using kinetic models applied to isolated rat hepatocytes. Drug Metab Dispos **36:**1365-1374.

Preiss D, Seshasai SR, Welsh P, Murphy SA, Ho JE, Waters DD, DeMicco DA, Barter P, Cannon CP, Sabatine MS, Braunwald E, Kastelein JJ, de Lemos JA, Blazing MA, Pedersen TR, Tikkanen MJ, Sattar N, and Ray KK (2011) Risk of incident diabetes with intensive-dose compared with moderate-dose statin therapy: a meta-analysis. JAMA **305:**2556-2564.

Rasool MF, Khalil F, and Laer S (2015) A physiologically based pharmacokinetic drug-disease model to predict carvedilol exposure in adult and paediatric heart failure patients by incorporating pathophysiological changes in hepatic and renal blood flows. Clin Pharmacokinet **54:**943-962.

Sattar N, Preiss D, Murray HM, Welsh P, Buckley BM, Craen AJd, McMurray JJ, Freeman DJ, and Jukema JW (2010) Statins and risk of incident diabetes: a collaborative meta-

analysis of randomised statin trials. Lancet **375:**735-742.

Shu N, Hu M, Liu C, Zhang M, Ling Z, Zhang J, Xu P, Zhong Z, Chen Y, Liu L, and Liu X (2016) Decreased exposure of atorvastatin in diabetic rats partly due to induction of hepatic Cyp3a and Oatp2. Xenobiotica **46:**875-881.

Smith NF, Figg WD, and Sparreboom A (2005) Role of the liver-specific transporters OATP1B1 and OATP1B3 in governing drug elimination. Expert Opin Drug Metab Toxicol **1:**429-445.

Takemoto K, ., Yamazaki H, ., Tanaka Y, ., Nakajima M, ., and Yokoi T, . (2003) Catalytic activities of cytochrome P450 enzymes and UDP-glucuronosyltransferases involved in drug metabolism in rat everted sacs and intestinal microsomes. Xenobiotica **33:**43-55.

Trudy R and Malcolm R (2006) Physiologically based pharmacokinetic modelling 2: predicting the tissue distribution of acids, very weak bases, neutrals and zwitterions. J Pharm Sci **95:**1238-1257.

Vildhede A, Karlgren M, Svedberg EK, Wisniewski JR, Lai Y, Noren A, and Artursson P (2014) Hepatic uptake of atorvastatin: influence of variability in transporter expression on uptake clearance and drug-drug interactions. Drug Metab Dispos **42:**1210-1218.

Wagle SR (1975) Critical evaluation of methods used for the isolation of rat liver hepatocytes for metabolic studies. Life Sci **17:**827-835.

Wang J, Xia S, Xue W, Wang D, Sai Y, Liu L, and Liu X (2013) A semi-physiologically-based pharmacokinetic model characterizing mechanism-based auto-inhibition to predict stereoselective pharmacokinetics of verapamil and its metabolite norverapamil in human. Eur J Pharm Sci **50:**290-302.

Watanabe T, Kusuhara H, Maeda K, Kanamaru H, Saito Y, Hu Z, and Sugiyama Y (2010) Investigation of the rate-determining process in the hepatic elimination of HMG-CoA reductase inhibitors in rats and humans. Drug Metab Dispos **38:**215-222.

Xu D, Li F, Zhang M, Zhang J, Liu C, Hu MY, Zhong ZY, Jia LL, Wang DW, Wu J, Liu L, and Liu XD (2014) Decreased exposure of simvastatin and simvastatin acid in a rat model of type 2 diabetes. Acta Pharmacol Sin **35:**1215-1225.

Yabe Y, Galetin A, and Houston JB (2011) Kinetic characterization of rat hepatic uptake of 16 actively transported drugs. Drug Metab Dispos **39:**1808-1814.

Yang J, Jamei M, Yeo KR, Tucker GT, and Rostami-Hodjegan A (2007) Prediction of intestinal first-pass drug metabolism. Curr Drug Metab **8:**676-684.

Yu S, Yu Y, Liu L, Wang X, Lu S, Liang Y, Liu X, Xie L, and Wang G (2010) Increased plasma exposures of five protoberberine alkaloids from Coptidis Rhizoma in streptozotocin-induced diabetic rats: is P-GP involved? Planta Med **76:**876-881.

Zhong ZY, Sun BB, Shu N, Xie QS, Tang XG, Ling ZL, Wang F, Zhao KJ, Xu P, Zhang M, Li Y, Chen Y, Liu L, Xia LZ, and Liu XD (2016) Ciprofloxacin blocked enterohepatic circulation of diclofenac and alleviated NSAID-induced enteropathy in rats partly by inhibiting intestinal beta-glucuronidase activity. Acta Pharmacol Sin **37:**1002-1012.

Footnotes

This study was supported by the National Natural Science Foundation of China [No 81573490, 81872930, 81473273 and 81673505], Natural Science Foundation of Jiangsu Province [BK20161457] and “Double First-Class” University project [CPU2018GY22].

DMD Fast Forward. Published on August 9, 2019 as DOI: 10.1124/dmd.118.085902
This article has not been copyedited and formatted. The final version may differ from this version.

Reprint requests:

Li Liu (liulee@yeah.net)

Center of Drug Metabolism and Pharmacokinetics, School of Pharmacy, China Pharmaceutical University, No.24 Tongjia Lane, Nanjing 210009, China.

[1]Xiaodong Liu and Li Liu are co-corresponding authors

Figure Legends

Figure 1. Schematic diagram of Semi-PBPK model involving both enzyme and transporter. A_i and Q_i indicated drug amount and blood flow in corresponding compartment, respectively. $CL_{int,gw,i}$ was intrinsic clearance in the i^{th} enterocyte compartment. K_i, $k_{a,i}$ and $k_{b,i}$ represented the transit rate constant, drug absorption rate constant and efflux rate constant from enterocyte to gut lumen, respectively. $CL_{up,ce}$, $CL_{ef,ce}$ and $CL_{h,met}$ were uptake clearance, efflux clearance and metabolic clearance in hepatocytes.

Figure 2. The expressions of Oatp1b2 (liver) or Oatp1a5 (intestine), P-gp, Bcrp and Cyp3a1 proteins in liver (A, B) and intestinal (C, D) of 10-day DM (A, C), 22-day DM (B, D), HFD and CON rats. Data are expressed as mean ± S.D. (n = 4) of CON, HFD and DM rats. $^{*}P < 0.05$, $^{**}P < 0.01$ versus CON rats ; $^{\#}P < 0.05$, $^{\#\#}P < 0.01$ versus HFD rats.

Figure 3. Intestinal permeability (P_{eff}) of Ator, rhodamine 123 and prazosin in the jejunum of 10-day DM (A, C, E), 22-day DM (B, D, F), HFD and CON rats using an in situ single-pass intestinal perfusion. Data are expressed as mean ± S.D. (n = 5) of CON, HFD and DM rats. $^{*}P < 0.05$, $^{**}P < 0.01$ versus CON rats ; $^{\#}P < 0.05$, $^{\#\#}P < 0.01$ versus HFD rats.

Figure 4. Uptake of Ator (A, B) and formation of O-OH-Ator (C, E) and P-OH-Ator (D, F) from Ator in hepatocytes of 10-day DM (A, C, E), 22-day DM (B, D, F), HFD and CON rats. Formation of 1'-hydroxymidazolam (G) and uptake of repaglinide (H) in hepatocytes of DM rats, HFD and CON rats. Data are expressed as mean ± S.D. (n = 5) of CON, HFD and DM rats. $^{*}P < 0.05$, $^{**}P < 0.01$ versus CON rats ; $^{\#}P < 0.05$, $^{\#\#}P < 0.01$ versus HFD rats.

Figure 5. The observed (points) and predicted (line) plasma concentrations of Ator after i.g.

Ator (10 mg/kg) to 10-day DM (A) and 22-day DM (B) rats or following i.v. Ator (2 mg/kg) to 22-day DM (C) rats. The relationship (D) of observed and predicted plasma concentration of Ator in experimental rats. Plasma concentrations of O-OH-Ator (E, F) and P-OH-Ator (G, H), as well as main pharmacokinetic parameters (inlet) following oral administration of Ator (10 mg/kg) to 10-day DM (E, G) and 22-day DM (F, H) rats. The observations for intravenous administration were cited from our previous report (Shu et al., 2016). Data are expressed as mean ± S.D. (n = 5) of CON, HFD and DM rats. $^{*}P < 0.05$,$^{**}P < 0.01$ versus CON rats ; $^{\#}P < 0.05$, $^{\#\#}P < 0.01$ versus HFD rats.

Figure 6. Predicted effects of Combination 1-5 on plasma concentration-time profiles of Ator following oral administration (10 mg/kg) to rats (A and B). Predicted plasma concentration-time profiles of Ator following oral administration (10 mg/kg) to 10-day DM and 22-day DM rats (C). Combination 1: decreases in intestinal P-gp and intestinal Cyp3a, expressions of other proteins were normal; Combination 2: increases in hepatic Cyp3a and Otap1b2, expressions of other proteins were normal; Combination 3: Combination 1+Combination 2, expression of Bcrp was normal; Combination 4: Combination 1+ Combination 2, and decreases in expression of intestinal Bcrp (mimicking 10-day DM rats); Combination 5: Combination 1+ Combination 2, and increases in expression of intestinal Bcrp (mimicking 22-day DM rats).

Tables

Table 1. Physiological and biochemical parameters in 10-day and 22-day rats following injection of streptozotocin (STZ) and or vehicle.

Parameters[a]	10-day			22-day		
	CON	HFD	DM	CON	HFD	DM
Body weight (g)	335.4±8.2	317.6±8.4	291.4±6.3**	368.4±5.2	383.6±7.3	301.4±5.4**
FBG (mM)	5.17±0.28	6.32±0.36*	21.69±2.31$^{**\#\#}$	5.64±0.36	6.51±0.57*	22.38±3.24$^{***\#\#\#}$
FINS (mIU/L)	32.17±5.34	34.31±6.51	36.21±4.76	31.06±4.21	32.24±3.25	35.34±3.78
HOMA-IR	8.21±1.41	9.63±1.84	36.69±2.43$^{**\#\#}$	7.89±1.13	9.52±1.56	35.41±2.54$^{***\#\#\#}$
TG (mM)	1.15±0.37	1.07±0.34	1.97±1.14$^{*\#}$	1.12±0.24	1.02±0.37	1.89±0.21$^{*\#}$
TC (mM)	2.14±0.14	2.69±0.42*	3.31±0.42**	2.21±0.57	2.58±0.91*	3.41±0.22**

[a]Data are expressed as mean ± S.D. (n = 5) of CON, HFD and DM rats.

$^{*}P < 0.05$, $^{**}P < 0.01$, and $^{***}P < 0.001$ versus CON rats; $^{\#}P < 0.05$, $^{\#\#}P < 0.01$ and $^{\#\#\#}P < 0.001$ versus HFD rats.

Table 2. Enzyme kinetic analysis of O-OH-Ator and P-OH-Ator from Ator in enzymatic incubations containing hepatic or intestinal microsomes of CON, HFD and DM rats. V_{max}, K_m and intrinsic clearance (CL_{int}) were calculated as described under Materials and Methods.

Parameters[a]	10-day			22-day		
	CON	HFD	DM	CON	HFD	DM
Liver						
O-OH-Ator						
K_m(μM)	6.09 ±0.64	7.79 ±0.77	4.44 ±1.13	6.32 ±0.38	7.26 ±0.31	6.33 ±0.29
V_{max}(pmol/min/mgprot)[b]	420.75 ±15.89	409.11 ±22.84	620.22 ±29.76$^{**\#\#}$	424.08 ±5.12	390.62 ±2.63**	599.07 ±5.52$^{**\#\#}$
CL_{int}(mL/min/mgprot)[b]	69.36 ±4.71	52.72 ±2.86**	144.76 ±31.85$^{**\#\#}$	67.27 ±4.82	53.9 ±2.64**	94.85 ±5.19$^{**\#\#}$
P-OH-Ator						
K_m(μM)	4.53 ±0.62	5.59 ±0.59	4.53 ±0.74	7.54 ±0.82	6.49 ±1.14	6.09 ±1.28
V_{max}(pmol/min/mgprot)[b]	195.31 ±8.33	184.86 ±6.97	289.44 ±12.74$^{**\#\#}$	307.3 ±0.95	280.98 ±12.53	383.1 ±58.71$^{**\#\#}$
CL_{int}(μL/min/mgprot)[b]	43.48 ±4.49	33.22 ±2.54**	64.73 ±7.2$^{**\#\#}$	41.11 ±4.58	44.08 ±6.5	63.47 ±4.27$^{**\#\#}$
Intestine						
O-OH-Ator						
K_m(μM)	11.23 ±1.02	11.56 ±0.72	11.81 ±0.83	11.19 ±1.53	11.25 ±0.69	10.79 ±1.28
V_{max}(nmol/min/mgprot)[b]	2.85 ±0.25	2.38 ±0.43	1.82 ±0.35$^{**\#\#}$	3.31 ±0.23	2.32 ±0.43*	1.61 ±0.35$^{**\#\#}$
CL_{int}(μL/min/mgprot)[b]	253.8 ±31.1	205.9 ±29.3	154.1 ±21.4$^{**\#\#}$	295.8 ±22.1	206.2 ±29.3*	149.2 ±18.3$^{**\#\#}$
P-OH-Ator						
K_m(μM)	11.34 ±1.09	10.98 ±1.34	11.71 ±1.98	11.95 ±1.05	10.75 ±1.3	9.79 ±1.74
V_{max}(nmol/min/mgprot)[b]	2.45 ±0.12	2.01 ±0.32	1.12 ±0.08$^{**\#\#}$	2.21 ±0.12	1.67 ±0.32*	0.95 ±0.08$^{**\#\#}$
CL_{int}(μL/min/mgprot)[b]	216.0 ±17.4	183.1 ±19.6	95.6 ±16.2$^{**\#\#}$	184.9 ±17.4	155.4 ±18.2*	97.0 ±12.2$^{**\#\#}$

[a]Data are expressed as mean ± S.D. (n = 5) of CON, HFD and DM rats.

[b]mg prot, mg protein.

$^{*}P < 0.05$, $^{**}P < 0.01$ versus CON rats; $^{\#}P < 0.05$, $^{\#\#}P < 0.01$ versus HFD rats.

Table 3. Formation of atorvastatin metabolism and uptake in hepatocytes of CON, HFD and DM rats. Related parameters were calculated as described under Materials and Methods.

Parameters[a]	10-day			22-day		
	CON	HFD	DM	CON	HFD	DM
O-OH-Ator						
V_{max} (pmol/min/10^6 cells)	111.5 ±15.42	93.66 ±8.19	99.83 ±3.33$^{*\#}$	60.28 ±5.55	72.05 ±4.78	93.25 ±7.93$^{**\#\#}$
K_m(μM)	53.8 ±12.1	24.13 ±4.55	7.5 ±0.79$^{**\#\#}$	8.31 ±2.34	7.29 ±1.54	5.51 ±1.62$^{**\#\#}$
CL_{int} (μL/min/10^6 cells)	2.07 ±0.31	3.88 ±0.32	13.31 ±0.17$^{**\#\#}$	7.25 ±0.42	9.88 ±0.51	16.92 ±0.23$^{**\#\#}$
P-OH-Ator						
V_{max} (pmol/min/10^6 cells)	23.48 ±2.31	29.27 ±1.77	43.41 ±1.02$^{**\#\#}$	29.38 ±2.33	37.44 ±2.99	48.78 ±1.52$^{**\#\#}$
K_m (μM)	10.14 ±2.87	7.51 ±1.43	5.52 ±0.44$^{*\#}$	4.98 ±1.38	5.14 ±1.43	3.21 ±1.38$^{**\#\#}$
CL_{int} (μL/min/10^6 cells)	2.31 ±0.25	3.89 ±0.31	7.86 ±0.62$^{**\#\#}$	5.91 ±0.27	6.92 ±0.34	15.19 ±0.51$^{**\#\#}$
Atorvastatin uptake						
V_{max} (pmol/min/10^6 cells)	396.84 ±32.75	375.5 ±11.75	660.69 ±10.18$^{**\#\#}$	342.79 ±5.88	387.88 ±8.63	731.85 ±39.39$^{**\#\#}$
K_m(μM)	6.81 ±0.79	3.41 ±0.23**	4.7 ±0.16$^{**\#\#}$	4.18 ±0.2	3.23 ±0.07	5.22 ±0.43$^{**\#\#}$
$CL_{up,int,Pas}$(μL/min/10^6 cells)	5.7 ±1.63	7.58 ±0.26	9.48 ±2.22	6.23 ±2.14	7.79 ±1.2	8.1 ±1.86
$CL_{up,int,active}$(μL/min/10^6 cells)	58.43 ±2.22	110.32 ±4.03**	140.81 ±3.3$^{**\#\#}$	82.14 ±2.84	120.04 ±2.08**	140.74 ±8.51$^{**\#\#}$
$CL_{int,uptake}$(μL/min/10^6 cells)	64.12 ±2.84	117.9 ±4.29**	150.28 ±3.52$^{**\#\#}$	88.37 ±2.98	127.82 ±2.28**	148.84 ±9.37$^{**\#\#}$

[a]Data are expressed as mean ± S.D. (n = 5) of CON, HFD and DM rats.

$^{*}P < 0.05$, $^{**}P < 0.01$ versus CON rats; $^{\#}P < 0.05$, $^{\#\#}P < 0.01$ versus HFD rats.

Table 4. The estimated and observed parameters of Ator in intestine and hepatocytes of 10-day DM, 22-day DM, HFD and CON rats.

Parameters	10-day			22-day		
	CON	HFD	DM	CON	HFD	DM
Intestinal transport						
$RE_{Oatp1a5}$[a]	1.00	0.86±0.13	0.38±0.13	1.00	1.48±0.24	0.54±0.20
$RE_{P\text{-}gp}$[a]	1.00	0.79±0.12	0.40±0.13	1.00	0.76±0.20	0.46±0.21
RE_{Bcrp}[a]	1.00	0.98±0.12	0.33±0.14	1.00	1.21±0.20	1.45±0.21
$P_{eff,Pas}$ ($\times 10^{-3}$cm/min)	11.95	11.95	11.95	12.02	12.02	12.02
$P_{eff,Oatp1a5}$ ($\times 10^{-3}$cm/min)[b]	0.80	0.69±0.10	0.30±0.10	0.77	1.14±0.18	0.42±0.15
$P_{eff,P\text{-}gp}$ ($\times 10^{-3}$cm/min)[b]	2.15	1.70±0.26	0.86±0.26	2.18	1.66±0.44	1.00±0.46
$P_{eff,Bcrp}$ ($\times 10^{-3}$cm/min)[b]	6.65	6.52±0.79	2.19±0.93	6.68	8.08±1.34	9.69±1.40
Pred P_{eff} ($\times 10^{-3}$cm/min)[c]	----	4.42±1.21	9.20±1.32	-----	3.42±1.35	1.75±1.37
Obs P_{eff} ($\times 10^{-3}$cm/min)[e]	3.95±0.67	4.81±0.46	7.16$^{**\#\#}$±0.72	3.92±0.77	5.34±0.83	1.53$^{**\#\#}$±0.82
Hepatic uptake						
$RE_{Oatp1b2}$[a]	1	1.51±0.20	1.97±0.26	1	1.07±0.25	1.93±0.23

$CL_{up,int,Pas}$ (μL/min/10^6 cells)	5.69	5.69	5.69	6.13	6.13	6.13
Pred$CL_{up,int,\ Oatp1b2}$(μL/min/10^6 cells)[b]	58.42	87.63±11.68	115.09±15.19	82.13	87.88±20.53	158.51±18.89
Pred$CL_{up,int}$ (μL/min/10^6 cells)[d]	-----	93.32±11.71	120.78±16.11	-----	94.01±21.32	164.64±22.13
Obs $CL_{up,int}$ (μL/min/10^6 cells)[e]	64.12±2.84	117.9±4.29**	150.28±3.52$^{**\#\#}$	88.37±2.88	127.82±2.28**	148.84±9.37$^{**\#\#}$

[a]RE:relatve expression of protein to CON rats;

[b]$P_{eff,i}$ (/or $CL_{up,i}$)=$P_{eff,,i}$ (/or $CL_{up,i}$)in normal rats×RE;

[c]Pred P_{eff}=$P_{eff,Pas}$+$P_{eff,Oatp1a5}$-$P_{eff,P\text{-}gp}$-$P_{eff,Bcrp}$;

[d]Pred $CL_{up,int}$=$CL_{up,int,Pas}$+$CL_{up,int,Oatp1b2}$.

[e]Data are expressed as mean ± S.D. (n = 5) of CON, HFD and DM rats.

$^{*}P < 0.05$, $^{**}P < 0.01$ versus CON rats; $^{\#}P < 0.05$, $^{\#\#}P < 0.01$ versus HFD rats.

DMD Fast Forward. Published on August 9, 2019 as DOI: 10.1124/dmd.118.085902
This article has not been copyedited and formatted. The final version may differ from this version.

Table 5. The physiological parameters of control and diabetic rats used in the semi-PBPK model

Parameters	Values		Units	Reference
	CON	DM		
Gastric emptying rate (k_0)	2.03	2.03	h^{-1}	(Kimura and Higaki, 2002)
Duodenum transit time (k_1)	28.75	28.75	h^{-1}	(Kimura and Higaki, 2002)
Jejunum transit time (k_2)	18.07	18.07	h^{-1}	(Kimura and Higaki, 2002)
Ileum transit time (k_3)	1.158	1.158	h^{-1}	(Kimura and Higaki, 2002)
Intestinal radius (r_1,r_2,r_3)	0.2	0.2	cm	(DeSesso and Jacobson, 2001)
Duodenum wall volume ($V_{1,gw}$)	1.08	1.08	mL	(Davies and Morris, 1993)
Jejunum wall volume ($V_{2,gw}$)	9.94	9.94	mL	(Davies and Morris, 1993)
Ileum wall volume ($V_{3,gw}$)	0.32	0.32	mL	(Davies and Morris, 1993)
Portal vein compartment volume (V_p)	0.25	0.25	mL	(Davies and Morris, 1993)
Liver blood compartment volume ($V_{h,b}$)	1.18	1.18	mL	(Davies and Morris, 1993)
hepatocyte compartment volume($V_{h,ce}$)	8.82	8.82	mL	(Davies and Morris, 1993)
Duodenum wall blood flow (Q_1)	0.972	2.223	mL/min	(Lucas and Foy, 1977; Hill and Larkins, 1989)
Jejunum wall blood flow (Q_2)	9.125	20.877	mL/min	(Lucas and Foy, 1977; Hill and Larkins, 1989)
Ileum wall blood flow (Q_3)	0.253	0.580	mL/min	(Lucas and Foy, 1977; Hill and Larkins, 1989)
Spleen and stomach blood flow (Q_4)	5.693	8.584	mL/min	(Lucas and Foy, 1977; Hill and Larkins, 1989)
Portal vein blood flow (Q_p)	16.043	32.264	mL/min	(Lucas and Foy, 1977; Hill and Larkins, 1989)
Hepatic artery blood flow ($Q_{h,at}$)	2.243	3.33	mL/min	(Lucas and Foy, 1977; Hill and Larkins, 1989)
Liver blood flow (Q_h)	18.286	35.594	mL/min	(Lucas and Foy, 1977; Hill and Larkins, 1989)
f_u	0.0567	0.0567	/	(Watanabe et al., 2010)
K_{ph}	2.42	2.42	/	(Trudy and Malcolm, 2006)
K_{pgut}	4.47	4.47	/	(Trudy and Malcolm, 2006)
Distribution volume (V_{c1})	1860	1860	mL/kg	(Shu et al., 2016)
Rate constant (k_{12})	0.018574	0.018574	min^{-1}	(Shu et al., 2016)
Rate constant (k_{21})	0.008159	0.008159	min^{-1}	(Shu et al., 2016)
Hepatic microsomal protein	44.8	44.8	mg /g liver	(Naritomi et al., 2003)
Intestinal microsomal protein	25.9	25.9	mg/g intestine	(Hatley et al., 2017)
Liver weight	40	36	g/kg body weight	(Lucas and Foy, 1977)
Number of hepatocytes	190×10^6	162×10^6	cells/g liver	(Wagle, 1975; Blomhoff et al., 1985)

Table 6. The predicted and observed pharmacokinetic parameters of Ator following i.g. Ator (10 mg/kg) to 10-day or 22-day DM, HFD and CON rats, and i.v. Ator (2 mg/kg) to 22-day DM, HFD and CON rats. Data were expressed as CON, HFD and DM rats. Observations for i.v. dose were cited from our previous report (Shu et al., 2016).

Parameters	CON		HFD		DM	
10-dayDM	Pred	Obs[a]	Pred	Obs[a]	Pred	Obs[a]
C_{max}(ng/mL)	108.90±15.64	91.52 ±6.18	119.16±14.72	110.45 ±46.24	167.04±15.92	149.64 ±85.84$^{**\#\#}$
T_{max}(min)	42.50±2.56	28.51 ±4.08	43.75±2.22	35.42 ±4.08	30.75±2.94	32.84 ±10.33
$AUC_{0-\infty}$(h ng/mL)	161.21±19.26	182.42 ±30.98	174.47±16.61	228.65 ±30.31	166.33±16.90	305.50 ±53.29$^{**\#\#}$
CL/F(mL/min/kg)	1048.23±128.25	860.39 ±14.98	964.08±97.93	691.053 ±19.72	1012.01±104.06	529.05 ±15.43$^{**\#\#}$
$T_{1/2}$(min)	109.98±0.54	79.48 ±30.41	110.07±0.39	76.54 ±18.06	96.43±0.24	68.67 ±97.07
MRT(min)	82.32±1.59	100.86 ±3.34	82.73±1.89	99.53 ±33.11	58.52±0.38	98.32 ±30.42
22-dayDM						
C_{max}(ng/mL)	125.22±13.2	101.77 ±14.86	160.56±12.35	131.10 ±36.56	55.59±17.04	59.61 ±10.81$^{**\#\#}$
T_{max}(min)	33.5±3.66	29.47 ±4.23	36.25±2.22	37.82 ±3.54	35.75±2.94	26.12 ±4.53
$AUC_{0-\infty}$(h ng/mL)	152.21±17.12	180.26 ±20.65	197.61±16.54	254.13 ±31.42	81.81±18.94	111.95 ±28.69$^{**\#\#}$
CL/F(mL/min/kg)	1108.51±127.61	875.44 ±15.79	849.16±73.1	631.38 ±17.39	2144.3±498.31	1375.62 ±17.35$^{**\#\#}$
$T_{1/2}$(min)	109.73±0.37	76.85 ±14.94	110.42±0.34	71.75 ±24.09	91.46±3.66	86.61 ±25.71
MRT(min)	73.42±0.5	97.31 ±21.29	74.38±0.46	95.27 ±22.22	74.55±3.38	101.91 ±35.88
Intravenousdose						
$AUC_{0-\infty}$(h ng/mL)	187.11±4.51	387.04 ±50.83	188.94±3.92	390.14 ±20.28	153.2±3.64	188.61 ±18.52$^{**\#\#}$
CL(mL/min/kg)	178.25±4.12	87.04 ±10.93	176.49±3.6	82.56 ±3.98	217.69±5.03	186.20 ±40.81$^{**\#\#}$
Vss(L/kg)	8.98±0.3	3.21 ±0.05	9.1±0.04	3.65 ±0.03	5.76±0.03	7.50 ±0.13$^{**\#\#}$
$T_{1/2}$(min)	111.38±0.71	134.00 ±22.00	111.59±0.65	124.00 ±27.00	98.31±0.37	115.00 ±16.00
MRT(min)	50.49±1.35	37.00 ±5.00	51.6±1.27	44.00 ±8.00	26.47±0.78	45.00 ±9.00

[a]Observation data (Obs) are expressed as mean ± S.D. (n = 5) of CON, HFD and DM rats.

$^{*}P < 0.05$, $^{**}P < 0.01$ versus CON rats; $^{\#}P < 0.05$, $^{\#\#}P < 0.01$ versus HFD rats.

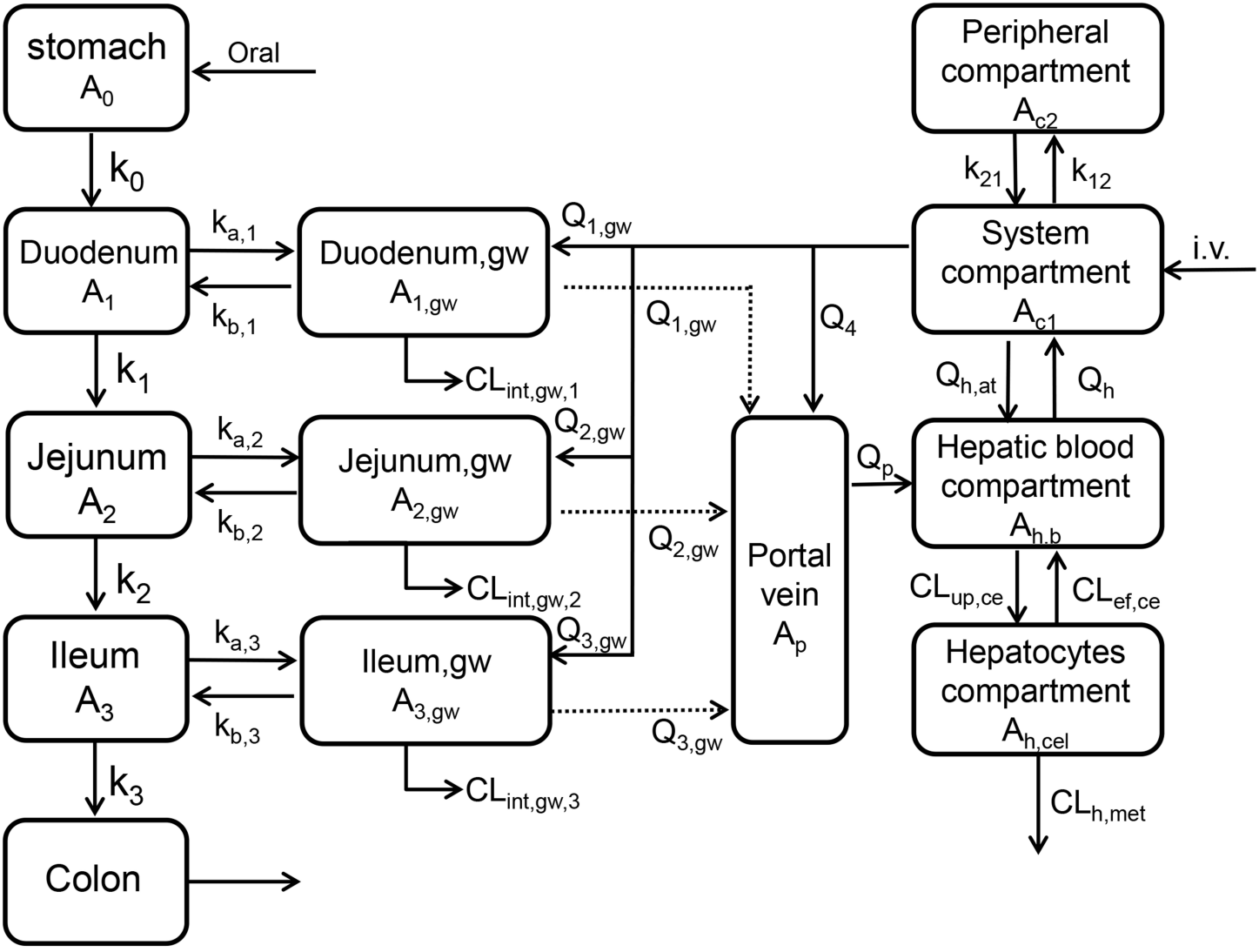
stomach
A_0
Oral
k_0
Duodenum
A_1
$k_{a,1}$
$k_{b,1}$
Duodenum,gw
$A_{1,gw}$
$CL_{int,gw,1}$
k_1
Jejunum
A_2
$k_{a,2}$
$k_{b,2}$
Jejunum,gw
$A_{2,gw}$
$CL_{int,gw,2}$
k_2
Ileum
A_3
$k_{a,3}$
$k_{b,3}$
Ileum,gw
$A_{3,gw}$
$CL_{int,gw,3}$
k_3
Colon
$Q_{1,gw}$
$Q_{2,gw}$
$Q_{3,gw}$
Q_4
Portal vein
A_p
Q_p
Peripheral compartment
A_{c2}
k_{21}
k_{12}
System compartment
A_{c1}
i.v.
$Q_{h,at}$
Q_h
Hepatic blood compartment
$A_{h,b}$
$CL_{up,ce}$
$CL_{ef,ce}$
Hepatocytes compartment
$A_{h,cel}$
$CL_{h,met}$

Fig.1

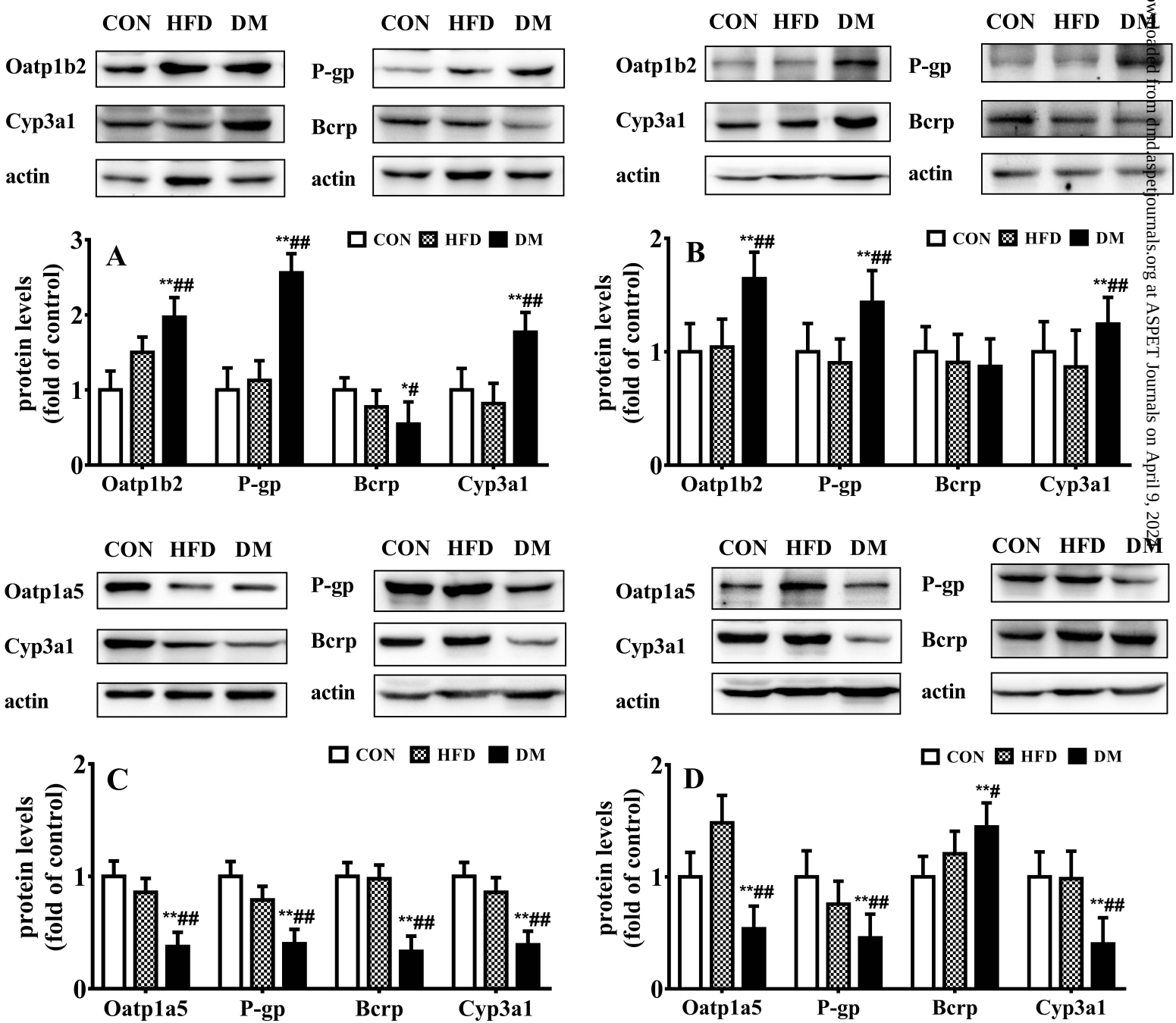

Fig.2

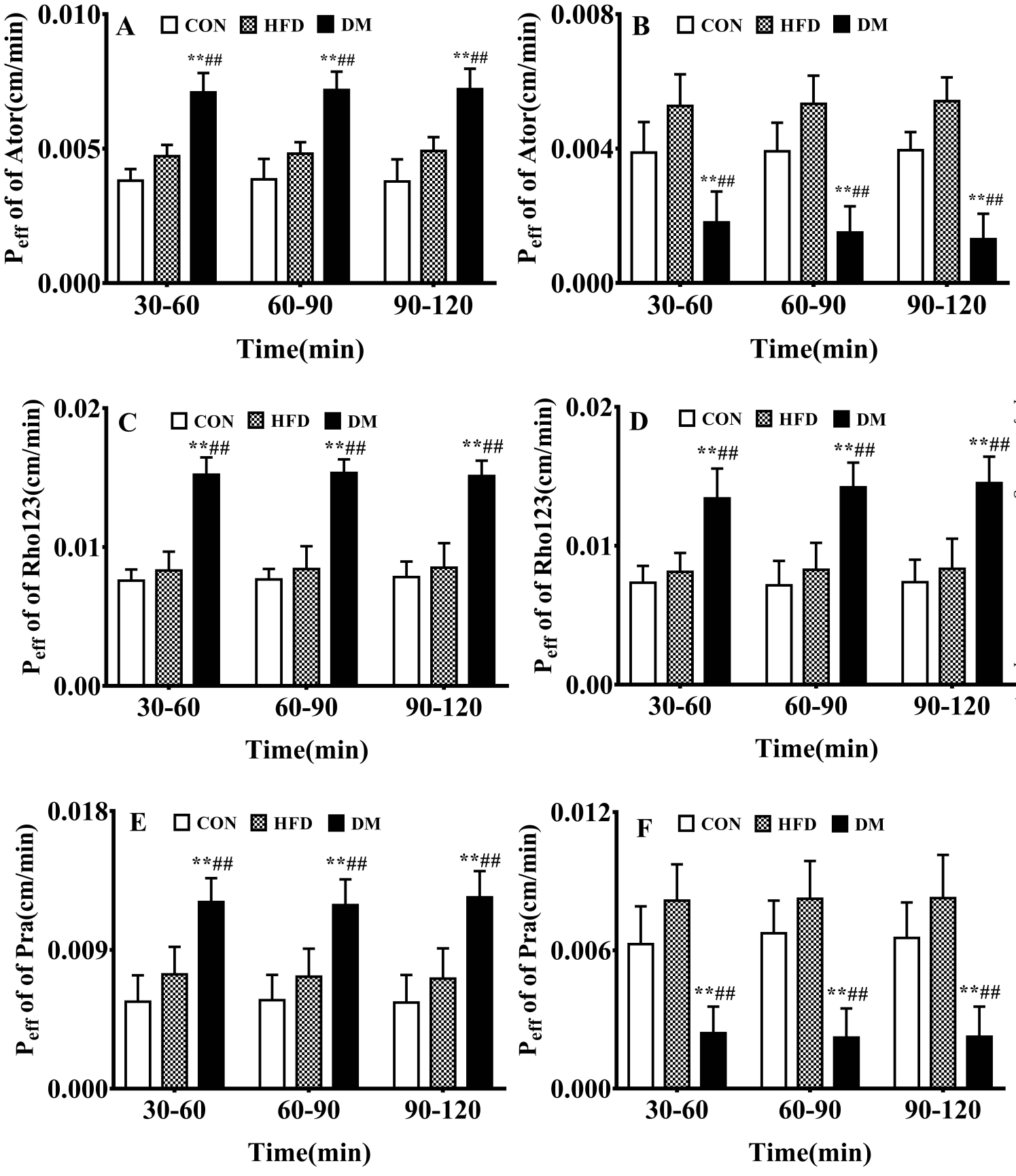

Fig.3

DMD Fast Forward. Published on August 9, 2019 as DOI: 10.1124/dmd.118.085902
This article has not been copyedited and formatted. The final version may differ from this version.

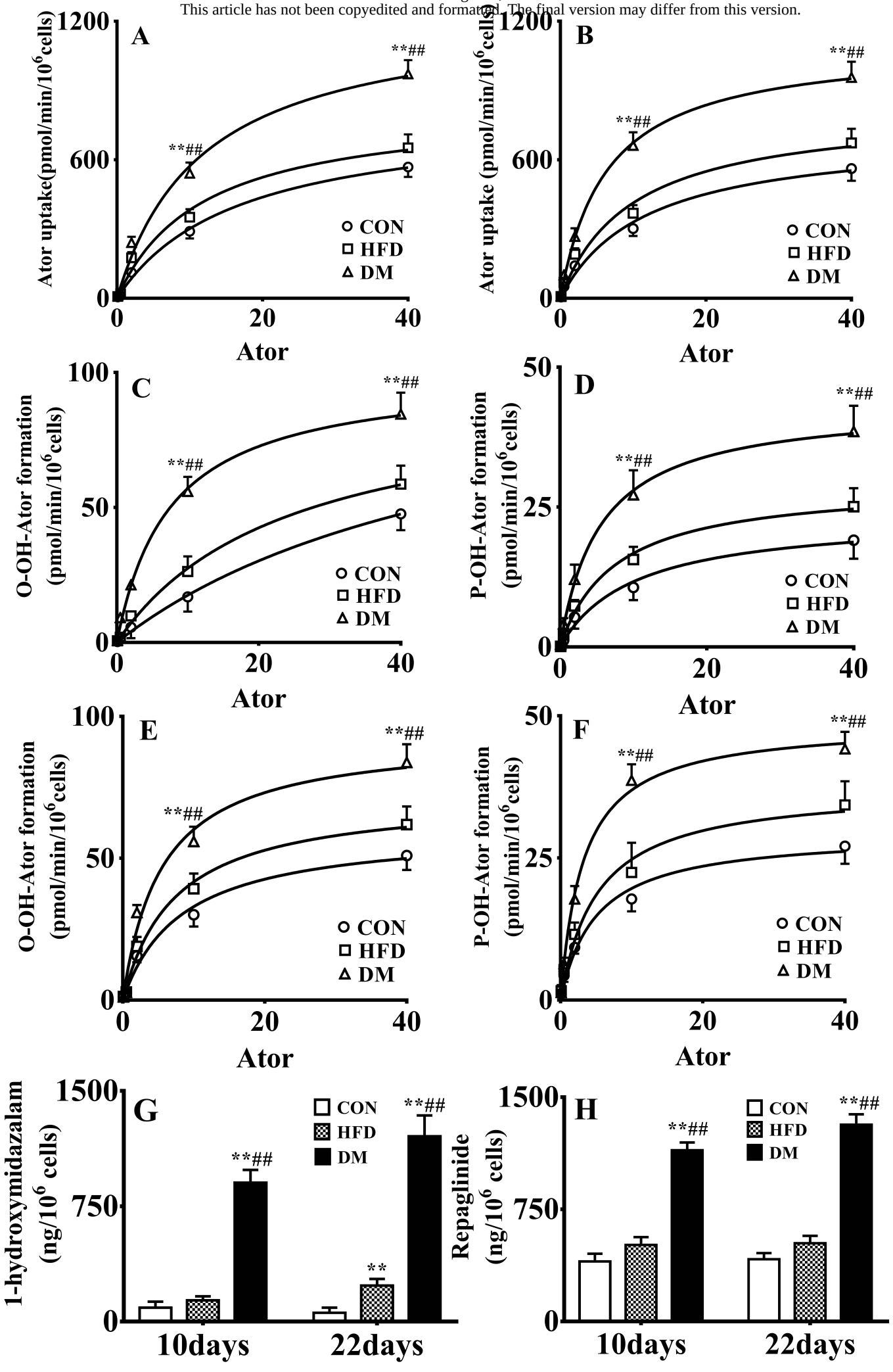

Fig.4

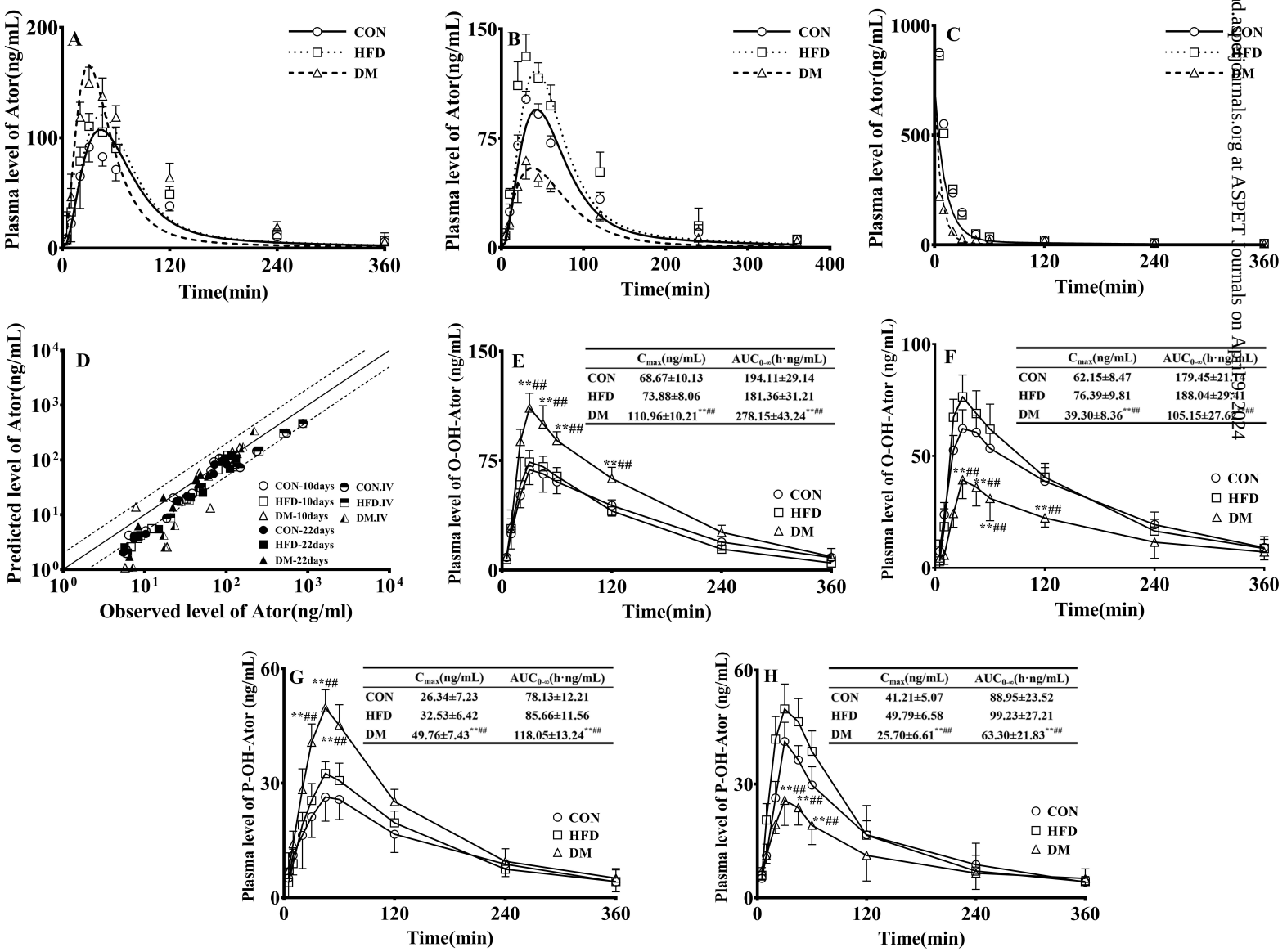

Fig.5

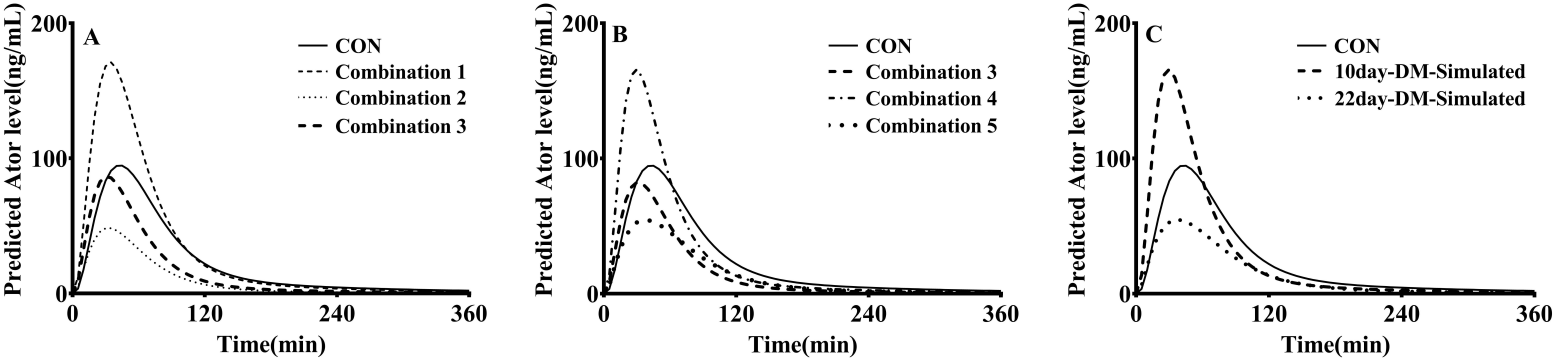
A
Predicted Ator level(ng/mL)
200
100
0
0
120
240
360
Time(min)
CON
Combination 1
Combination 2
Combination 3
B
Predicted Ator level(ng/mL)
200
100
0
0
120
240
360
Time(min)
CON
Combination 3
Combination 4
Combination 5
C
Predicted Ator level(ng/mL)
200
100
0
0
120
240
360
Time(min)
CON
10day-DM-Simulated
22day-DM-Simulated

Fig.6

Supplemental Information

Prediction of atorvastatin pharmacokinetics in high-fat diet and low-dose streptozotocin induced diabetic rats using a semi-physiologically based pharmacokinetic model involving both enzyme and transporter turnover

Zhongjian Wang, Hanyu Yang, Jiong Xu, Kaijing Zhao, Yang Chen, Limin Liang, Ping Li, Nan Chen, Donghao Geng, Xiangping Zhang, Xiaodong Liu and Li Liu.

Center of Drug Metabolism and Pharmacokinetics, School of Pharmacy, China Pharmaceutical University, Nanjing, China. (Z.W., H.Y., J.X., K.Z., Y.C., L.L., P.L., N.C., D.G., X.Z., X.L., L.L.)

Supplemental methods:

Development of DM rats

DM rats were induced by high fat diet feeding plus low dose STZ intraperitoneal injection according to the method described previously (Shu et al., 2016). Briefly, the rats (weighing 100-120 g) were divided into CON, HFD and DM rats. The CON rats were fed on normal chow while both HFD rats and DM rats were fed on high fat diet for 8 weeks (TROPHIC Animal Feed High-tech Co. Ltd, Nantong, China). The high fat diet consisted of 15% lard (w/w), 5% sesame oil, 20% sucrose, 2.5% cholesterol and 57.5% normal chow. Following 8-week of dietary manipulation, DM rats intraperitoneally received a single dose of STZ (35 mg/kg) intraperitoneal injection. Other rats only received vehicle. On day 7 following vehicle or STZ injection, fasting blood glucose was measured on a glucometer (AccuChek Performa, Roche Diagnostics, Indiana, USA). Only rats with fasting blood glucose level higher than 11.1 mM were considered as successful DM rats.

Intestinal absorption of Ator in rats

In situ single-pass intestinal perfusion experiments were performed to evaluate intestinal absorption of Ator as well as functions of intestinal P-gp and Bcrp in DM rats . In brief, the experimental rats, fasted overnight, received intraperitoneal injection of 45 mg/kg pentobarbital sodium salt (dissolved in 0.9% saline solution). A midline abdominal incision was made and the small intestine was exposed. The jejunum (10 cm) was isolated and flushed with 10 mL of saline pre-warmed to 37 ℃ to reach a steady state. The manipulation should be performed carefully in order to minimize the surgery and to maintain an intact blood supply.

Western blot analysis

The protein levels of P-gp, Bcrp, Oatp1b2, Oatp1a5 and Cyp3a1 in liver and intestine of

rats were measured by western blotting. Briefly, the rat hepatic and intestinal tissues were homogenized and lysed in RIPA lysis buffer in appropriate proportion. The protein concentrations of tissue and cell lysates were measured by the BCA protein assay kit. Equal amounts of proteins were subjected to sodium dodecyl sulfate-polyacrylamide gel electrophoresis and transferred to polyvinylidene fluoride membranes (Millipore Corporation, Billerica, MA, USA). Blots were blocked for 2 h in 5% non-fat dry milk-Tris-buffered saline-0.1% Tween 20. The membranes were then incubated with primary antibodies P-gp (1:500), Bcrp (1:500), Oatp1b2 (1:200), Oatp1a5 (1:200), Cyp3a1 (1:500) or β-actin (1:1000) overnight at 4℃, followed by a horseradish peroxidase-conjugated secondary anti-rabbit antibody (1:5000) for P-gp, Bcrp, Oatp1b2, Oatp1a5 and β-actin or anti-mouse antibody (1:5000) for Cyp3a1 for 2 h at room temperature. The immunoreactivity was detected using SuperSignal West Femto Chemiluminescent Substrate (Thermo Fisher Scientific Inc., Rockford, IL USA) by a gel imaging system (ChemiScope 2850, Clinx Science Instruments Co., Ltd., Shanghai, China).

Supplemental Figures:

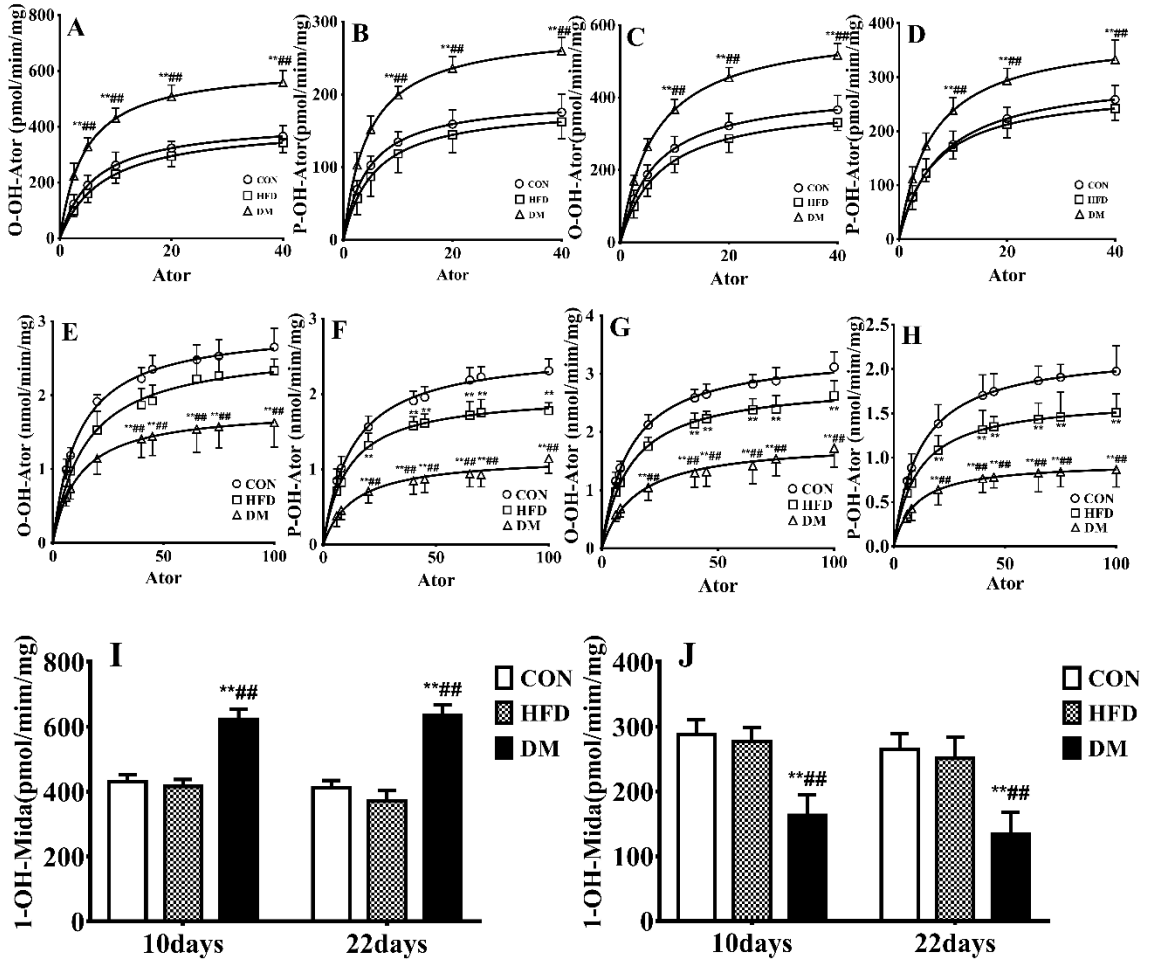

Supplemental Figure 1

Supplemental Figure 1. Formation kinetics of O-OH-Ator (A, C) and P-OH-Ator (B, D) from Ator in hepatic microsomes of 10-day DM (A, B), 22-day DM (C, D), HFD and CON rats; O-OH-Ator (E, G) and (F, H) in intestinal microsomes of 10-day DM (E, F), 22-day DM (G, H), HFD and CON rats; Formation kinetics of 1'-OH-Midazolam from Midazolam in hepatic (I) and intestinal (J) microsomes of 10-day DM, 22-day DM, HFD and CON rats; Data are expressed as mean ± S.D. (n = 4) of CON, HFD and DM rats. $^{*}P < 0.05$, $^{**}P < 0.01$ versus CON rats ; $^{\#}P < 0.05$, $^{\#\#}P < 0.01$ versus HFD rats.

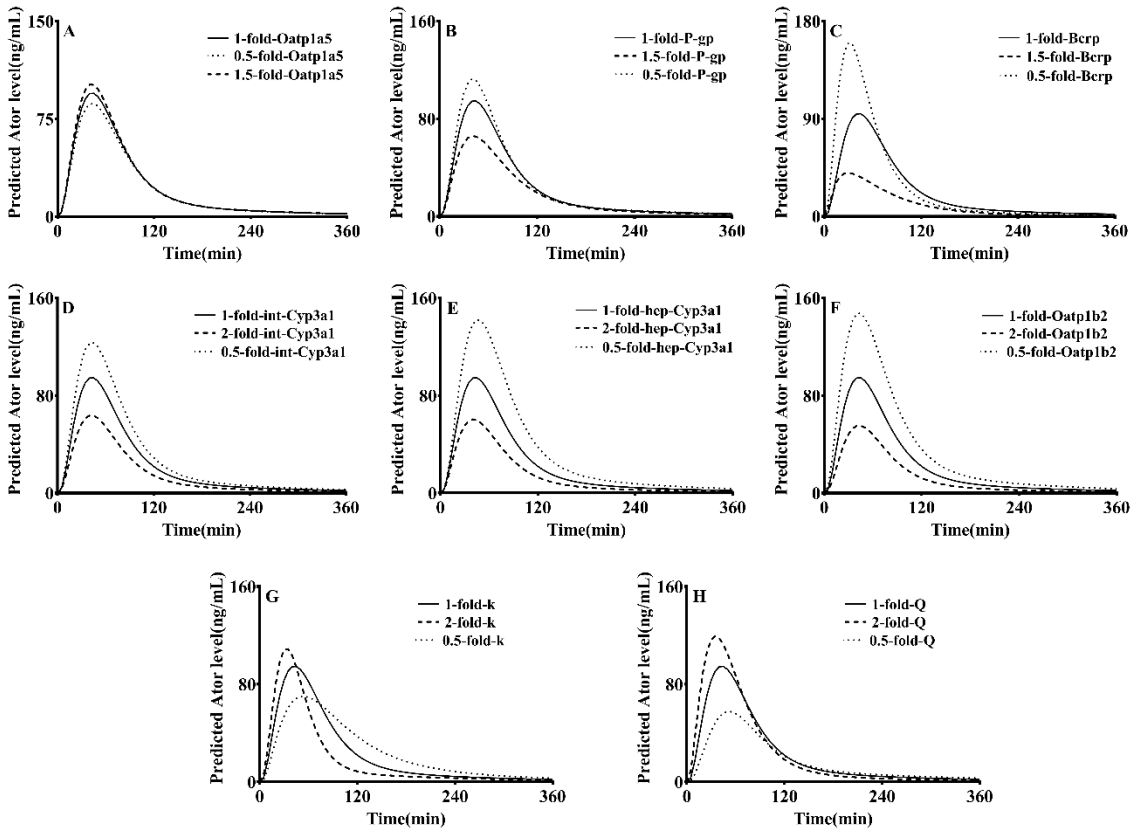

Supplemental Figure 2

Supplemental Figure 2. Predicted effects of variations in intestinal Oatp1a5 (A), intestinal P-gp (B), intestinal Bcrp (C), intestinal Cyp3a (D), hepatic Cyp3a (E), hepatic Oatp1b2 (F), gastrointestinal transit rate constant k (G) and organ blood flow rate Q (H) on plasma concentration-time profiles of Ator following oral administration (10 mg/kg) to rats.

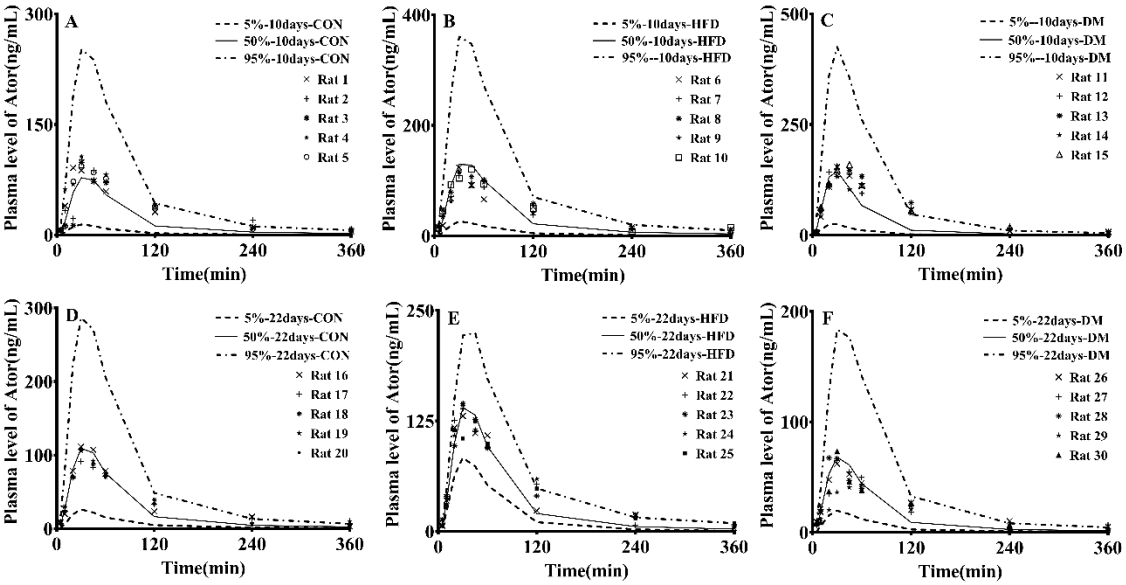

Supplemental Figure 3

Supplemental Figure 3. The visual predictive checks of predicted plasma concentration-time profiles of 10 mg/kg atorvastatin in CON, HFD and DM rats (n=5).10-day CON rats (A), 10-day HFD rats (B), 10-day DM rats (C), 22-day CON rats (D), 22-day HFD rats (E) and 22-day DM rats (F)